https://doi.org/10.5194/egusphere-2025-6451
Preprint. Discussion started: 13 January 2026

Understanding Soil Organic Carbon Dynamics in Integrated Crop-Pasture Systems: Insights into Deep Carbon

Maximiliano González-Sosa[1,2], Carlos A. Sierra[2], Juan A. Quincke[3], Walter E. Baethgen[4], Susan Trumbore[2], M. Virginia Pravia[5, 2]

[1] Universidad de la República, Facultad de Agronomía, Departamento de Suelos y Aguas, Montevideo, Uruguay.
[2] Department of Biogeochemical Processes (BGP), Max Planck Institute for Biogeochemistry, Jena, Germany
[3] Instituto Nacional de Investigación Agropecuaria, INIA - La Estanzuela, Colonia, Uruguay
[4] International Research Institute for Climate and Society, Columbia Climate School, Columbia University, New York City, New York, USA
[5] Instituto Nacional de Investigación Agropecuaria, INIA – Treinta y Tres, Treinta y Tres, Uruguay

Correspondence to: Maximiliano González-Sosa (mgonzalez@fagro.edu.uy)

Abstract. In soils from a long-term agricultural experiment (LTE) installed in Uruguay, integrated crop-pasture rotational systems promote greater soil organic carbon (SOC) accumulation than continuous cropping systems at the soil surface (0-20 cm) by avoiding losses of centennial C. Here, we explore whether old C losses due to continuous cropping extend to deeper layers or whether other factors control deep carbon dynamics in the same LTE in Uruguay. To answer this question, we analyzed the vertical profile of SOC, $\Delta^{14}C$ and $\delta^{13}C$ in fractions representing compartments of different stability at two points in time of two contrasting agricultural treatments (continuous cropping and integrated crop-pasture rotational system). Additionally, using site-specific data we fit dynamic compartmental models to describe the temporal trajectory of C stocks and $\Delta^{14}C$ signature in the stable SOC fractions at depth on the integrated crop-pasture system. Based on these models, we used the estimated age distribution for soil C to assess whether it is possible to sequester C in these compartments on time scales relevant in terms of climate change mitigation. We found that the SOC fractions associated with the mineral phase (MAOM - HF) are highly isolated with respect to inputs of recent atmospheric CO_2 and that this isolation increases substantially with depth in the soil profile. This degree of isolation was characterized by a progressive increase in the difference between $\Delta^{14}C$ profile between MAOM-HF and LF-POM (more labile) fractions with depth. The differences found in the C stock between management systems could be explained by different losses of old legacy C and the high stability and isolation of the compartments associated with the mineral phase in the crop-pasture rotational system. The high stability of MAOM-HF in this agricultural system was reflected in the very old ages of these C pools, from approximately 700 years at surface to a value of several thousand years at depth. The inclusion of a vertical transfer mechanism for previously stabilized material was not necessary to explain the general age structure and the capacity of these systems to sequester new C inputs in deep stable layers. The results of this work imply that integrated crop-pasture rotational systems have not been able to sequester significant amounts of new C along the profile (and in particular at depth), although they are relevant to preserve the natural C legacy of these soils.

https://doi.org/10.5194/egusphere-2025-6451
Preprint. Discussion started: 13 January 2026

1 Introduction

There is great interest in the scientific community to develop agricultural technologies that can maintain or increase soil organic carbon (SOC) and achieve positive impacts in terms of climate change mitigation (Cates et al., 2016; Rui et al., 2022). This is crucial in a scenario of global temperature rise due to greenhouse gas emissions (IPCC, 2014, 2022). In turn, changes in the amount of SOC have not only potential climatic impacts, but the increases in SOC concentration also determine the improvement of soil properties such as fertility, erosion control, water retention capacity and infiltration, thus affecting its agricultural productivity (Lal, 1993; Rubio et al., 2019).

SOC does not behave as a homogeneous pool (Cotrufo et al., 2015; Schmidt et al., 2011; Trumbore, 2009), and it is widely accepted that modeling its dynamics with homogeneous kinetics can lead to significant overestimation errors of the SOC response on timescales of decades to centuries (Schuur et al., 2016; Trumbore, 2009). Traditionally, chemical recalcitrance of soil organic compounds has been considered the primary factor responsible for SOC stability. However, this concept has recently been strongly challenged by a large body of evidence which shows that all SOC is potentially degradable and that even simple and labile compounds can have high ^{14}C ages (Kleber et al., 2011). In this paradigm shift, it has been proposed that the association of soil C with the mineral phase through sorption processes is the main factor in soil C stabilization (Schmidt et al., 2011). Another mechanism that has been reported to be responsible for increased C stability is the formation of soil aggregates, as the complex geometry of soil porosity determines that part of the SOC is located in places where microbial enzymatic action is hindered and oxygen diffusion is slowed down (Chevallier et al., 2010; Keiluweit et al., 2017). A final mechanism is through the increased physical isolation of organic compounds from living microbes, especially in deep soils where microbial biomass declines as does carbon content (Don et al., 2013).

Separation of soil organic matter into compartments of different stability is required to correctly understand and model SOC dynamics (Jenkinson, 1990). Various techniques for partitioning SOC fractions have been applied as a proxy to differentiate C pools with contrasting kinetics (Poeplau et al., 2018), with physical methods of particle size or density separation being the most widely used (Cambardella and Elliott, 1992; Golchin et al., 1994; Six et al., 2002). Regarding the size fractionation technique (Cambardella and Elliott, 1992), in most cases two fractions are separated, particulate organic matter (POM) and mineral-associated organic matter (MAOM). POM is largely comprised of poorly transformed plant fragments, whereas MAOM is composed of low molecular weight compounds with a higher degree of microbial transformation that are adsorbed to the mineral phase, giving them a longer persistence in the soil (Lavallee et al., 2020). Another widely used fractionation technique is density separation (Golchin et al., 1994; Schrumpf et al., 2013; Sohi et al., 2001). This technique separates the soil organic matter associated with the mineral phase (heavy fraction, HF) from the particulate (light fraction, LF) material inside (occluded light fraction, oLF) and outside aggregates (free light fraction, fLF), characterizing both the stabilization by association with the mineral phase (physicochemical protection) and by aggregates formation (physical protection).

https://doi.org/10.5194/egusphere-2025-6451
Preprint. Discussion started: 13 January 2026

Characterization of the relative abundance of "rare" C isotopes (^{14}C and ^{13}C) in different SOC fractions and respired CO_2 has been widely used as a proxy to understand the turnover time of each of these fractions and to assess whether the separation method is effective in generating compartments that are functionally and kinetically contrasting (Balesdent et al., 1987, 2018; Poeplau et al., 2018; Trumbore and Zheng, 1996). Particularly, soil radiocarbon data is a useful tool for understanding C dynamics in terrestrial systems (and in different soil fractions) (Torn et al., 2009; Trumbore, 2000). Radiocarbon is a measure of the time that has elapsed since the photosynthetic fixation of CO_2 from the atmosphere. In particular, due to the radiocarbon peak that occurred around 1960, ^{14}C is an extremely useful isotopic tracer for understanding the rates at which the biosphere (and especially the soil) exchanges C with the atmosphere (Trumbore, 2009). In turn, the $\delta^{13}C$ isotopic signature can be used as a proxy to characterize the degree of microbial processing of SOC, due to the existence of a ^{13}C enrichment of the microbial biomass with respect to the input plant substrate (ŠantRůČková et al., 2000; Wynn et al., 2005), determining that those C compartments with a higher proportion of C of microbial origin are more enriched in this isotope.

Several studies have shown that it is possible to maintain or even increase the SOC content of agricultural soils in temperate regions through the application of certain crop management practices (González-Sosa et al., 2024; Rui et al., 2022; Xu et al., 2020). For example, management practices such as reduced tillage, diversification of agricultural sequences, and application of organic amendments have been shown to be effective in increasing the content of labile organic matter (i.e., POM or LF). However, their effectiveness in promoting SOC accumulation in more persistent compartments (i.e., MAOM or HF) has been debated (Castellano et al., 2015; Rui et al., 2022). Particularly, the inclusion of perennial pastures in agricultural rotations represents a sustainable intensification strategy capable of maintaining or increasing SOC stocks without compromising the productivity of the systems (Baethgen et al., 2021; Pravia et al., 2019). Although efforts have been made to generate an initial approximation of the effect of these management practices on SOC stock and its stability at depth in the soil profile (Gentile et al., 2005), there is still a need to deepen knowledge on this subject. Contributing to reduce this knowledge gap, it is important in the context of initiatives such as the '4 per 1000' (Minasny et al., 2017), which proposes to increase C concentrations to a depth of 2 meters on a global scale, an assumption that has been debated (Rumpel et al., 2019) because there is no consensus in the literature on the actual capacity of deep soil layers to behave as sufficiently active to store new C on short time scales. As Trumbore (2000) claims, not all soil carbon interacts with the atmosphere on the same time scale, and this is particularly true when we assess it in deep layers.

Deep SOC would have high stability because it has generally been reported with ages ranging on the order of centuries to millennia (Mathieu et al., 2015; Rumpel and Kögel-Knabner, 2011; Van Der Voort et al., 2019). This is explained by a more rapid decrease in labile C compartments at depth (POM, LF) compared to stable compartments (MAOM, HF) (Galluzzi et al., 2025; Salvo et al., 2010) and by low decomposition rates that are compensated by low inputs to result in the relatively low SOC concentrations that are typical of deep layers (Von Fromm et al., 2024). These low decay rates are due to the higher intensity of stabilization mechanisms that would increase at depth (Rumpel and Kögel-Knabner, 2011). Kaiser and Kalbitz (2012) also state that a mechanism that could determine older C ages at depth could be desorption and vertical movement of pre-aged organic C in the form of dissolved organic carbon (DOC). However, this latter mechanism has been

https://doi.org/10.5194/egusphere-2025-6451
Preprint. Discussion started: 13 January 2026

called into question by the findings of Sierra et al. (2024), who suggest that vertical movement in the form of diffusion and advection processes seem to be of secondary importance in determining the vertical profile of SOC and ^{14}C and that the essential process is the net balance between inputs and decomposition at each layer (determined mostly by root inputs and microbial decomposition).

Previous work carried out at the same experimental site as the present work (González-Sosa et al., 2024), based on C stocks in size fractions and radiocarbon measurements in soil and incubations, estimated the compartment containing most of the organic carbon (MAOM) at the surface (0-20 cm) to be highly stable in temperate soils under the conservationist management practice of integrated crop-pasture rotational systems. These results suggest that there is an important decoupling between the dominant compartment of SOC and the atmospheric C pool used to produce fresh plant organic matter inputs. In this work, we aim to expand upon these initial findings by characterizing the effect of the inclusion of perennial pastures in agricultural rotations on deep SOC dynamics.

We hypothesize that soils under crop-pasture rotational systems have higher C stocks than continuous cropping systems throughout the profile, including deep horizons. This higher deep SOC stock is caused by the elevated persistence of C associated with the soil's mineral phase due to the preservation of very old SOC with high microbial reprocessing and not due to new C sequestration. The confirmation of this process would be evidenced by highly negative $\Delta^{14}C$ isotopic signatures and high ^{13}C enrichment (higher $\delta^{13}C$ values) in the C compartments associated with the mineral fraction at deep layers. Additionally, we hypothesize that the consideration of vertical flows of pre-aged C are not necessary to explain the older ages of C at depth. Soil C dynamics and aging in the profile were evaluated using a dynamic compartmental model (Sierra et al., 2012, 2014) with which we evaluated the effect of changing inputs over time and considering different intensities of vertical movement of old C on its ^{14}C signature, age and transit time of C in the system.

To test our hypotheses, we will focus on answering the following guiding questions:

1. Do integrated crop-pasture systems constitute an agronomic strategy that enhances the sequestration of mineral-associated C (MAOM-HF) in deep layers compared to systems that include only annual crops?
2. Does a significant incorporation of recent mineral-associated C occur in deep layers within these productive systems?
3. Is there a higher microbial reprocessing in the mineral-associated C at depth?
4. Is it necessary to consider a vertical flow of pre-aged C to understand the vertical age profile of mineral-associated C?

https://doi.org/10.5194/egusphere-2025-6451
Preprint. Discussion started: 13 January 2026

2. Materials and methods

2.1. Experimental site and long-term experiment (LTE)

The study was carried out at the long-term experiment (LTE) of the research station "La Estanzuela" of the National Institute of Agricultural Research of Uruguay (INIA). The site is located in southwestern Uruguay (Colonia, Uruguay; 34°20′33″ S, 57°43′25′25″ W), in the center of the Río de la Plata Grassland ecoregion (Baeza et al., 2022). The mean annual cumulative precipitation is 1126.7 (±269.9) mm and the cumulative reference evapotranspiration is 1192.5 (±74.3) mm based on 53 years of meteorological records (Fig. 1a). Rainfall is strongly variable between years, although no changing trends are observed over time (Fig. 1b). The mean annual temperature reaches 16.9 °C, showing a marked seasonality. On average, monthly maximum temperatures are 29.0 °C in January and 14.8 °C in July, while monthly minimum temperatures average 17.8 °C and 6.2 °C for the same months, respectively (Fig. 1a).

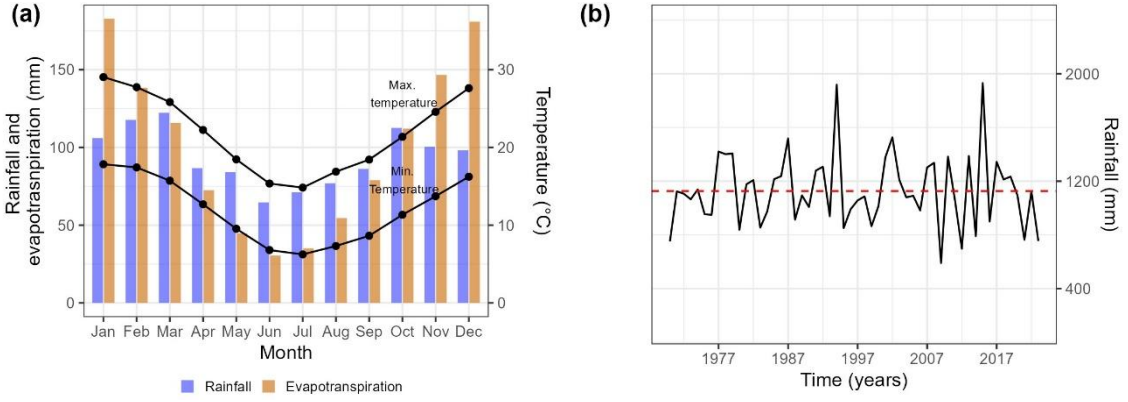

Figure 1. Monthly distribution of mean accumulated rainfall and evapotranspiration (left Y axis, bars) and monthly mean maximum and minimum temperature (right Y axis, lines) (a); time series of annual accumulated rainfall (mm) (dotted red line corresponds to the time series average) (b). The information derives from a 53-year time series (1969 – 2022) provided by INIA's meteorological stations (INIA GRAS, 2023). Reprinted from González-Sosa et al. (2024), *SOIL*, licensed under Creative Commons Attribution 4.0 International (CC BY 4.0).

The geomorphology of the site is characterized by the presence of rolling hills with average slopes of approximately 3%. The soil is classified as a fine, smectitic Vertic Argiudoll based on the USDA taxonomy system (Soil Survey Staff, 2014). Detailed soil information from a previous sampling conducted at the experimental site is presented in Table 1, which shows a slightly acidic soil with a well-developed Bt horizon and no rockiness.

https://doi.org/10.5194/egusphere-2025-6451
Preprint. Discussion started: 13 January 2026

Table 1. La Estanzuela LTE soil characteristics[(a)]

Horizon	A_p	B_{t1}	B_{t2}	B_{t3}
Depth (cm)	0-30	30-42	42-72	72-97
Clay (g kg^{-1})	287	472	500	466
Silt (g kg^{-1})	637	466	461	486
Sand (g kg^{-1})	76	62	39	48
pH (KCl)	5.6	5.6	5.2	5.5
SOC (g kg^{-1})	20.8	7.8	9.5	1.3
N_{tot} (g kg^{-1})	1.7	0.8	0.7	0.4
CEC_e ($cmol_c$ kg^{-1})	17.1	22.9	24.4	27.1
CEC_{pH7} ($cmol_c$ kg^{-1})	20.6	25.5	26.6	28.4

Note: CECe: efective Cation Exchange Capacity. Information obtained from a soil mapping conducted by the Uruguayan Ministry of Agriculture in 1985.
[(a)]Reprinted from González-Sosa et al. (2024), *SOIL*, licensed under Creative Commons Attribution 4.0 International (CC BY 4.0).

The INIA La Estanzuela LTE, installed in 1963, is the oldest long-term agricultural experiment in Latin America and one of the oldest in the world. This LTE evaluates the effects on soil properties and crop productivity of a gradient of seven treatments of varied agricultural intensity, from continuous cropping agriculture with and without fertilizer application to integrated crop-pastures systems. It has a randomized complete block design with three replications and each plot has an area of 0.5 ha. The installation of crops and pastures is currently carried out in a no-till farming system. However, this technology has been adopted in recent decades, and tillage was implemented in land preparation previously (Baethgen et al., 2021; González-Sosa et al., 2024). A detailed description of the experimental site and the LTE can be found in several previous works, such as Baethgen et al. (2021), González-Sosa et al. (2024) and Grahmann et al. (2020).

Two of the seven experimental treatments were selected for this work because of their contrasting effects on SOC dynamics: a continuous cropping system (CC) and an integrated crop-pasture rotation system (R) with 50% of the time dedicated to grain crop production and 50% to perennial pastures. The current crop rotation of the CC system has two winter crops (barley and wheat) and three summer crops (maize, sorghum and soybeans) that are fit in three years as follows: maize (yr 1), barley and sorghum double-cropping (yr 2), wheat and soybeans double-cropping (yr 3). On the other hand, the R system consists of three years of the same sequence as the CC system in rotation with three years of a perennial pasture of white clover, bird's-foot trefoil, and tall fescue. The rotations have undergone slight modifications in the crops grown throughout the history of the LTE, intending to adapt the technologies represented in the experiment to changes in agricultural management practices that have occurred in real farming systems throughout the years. A detailed description of this historical evolution can be found in González-Sosa et al. (2024) and Quincke et al. (2019).

https://doi.org/10.5194/egusphere-2025-6451
Preprint. Discussion started: 13 January 2026

2.2. Soil sampling and analysis

Stratified soil sampling was carried out in 2008 and 2021 in the plots corresponding to the CC and R treatments of the LTE. The stratification scheme used was as follows: 0-10 cm, 10-20 cm, 20-40 cm, 40-60 cm and 60-80 cm. The soil samples were sieved to less than 2 mm and a subsample was dried at 40 °C and finely ground to be analyzed for C content by dry combustion (Elementar Vario Max) at the Max-Planck Institute for Biogeochemistry (MPI-BGC, Jena-Germany). The samples extracted in 2021 were fractionated, separating sand-size SOC or particulate organic matter (POM) (> 53 µm) from silt plus clay SOC or mineral associated organic matter (MAOM) (< 53 µm) based on the technique described by Cambardella and Elliott (1992). Both fractions were dried at 40 °C and finely ground to be analyzed for $\delta^{13}C$ signature by isotope ratio mass spectrometry (IRMS) and $\Delta^{14}C$ by accelerator mass spectrometry (AMS) at MPI-BGC. Additionally, the C content of POM was obtained by dry combustion. Undisturbed soil samples were taken in 2021 for bulk density determination which were used for SOC stock calculations. Particularly, POM C stock was calculated considering its C concentration and recovered weight while MAOM C stock was calculated as the difference between SOC and POM C stock. All SOC stocks were expressed in Mg ha^{-1}.

The samples extracted in 2021 were incubated to obtain $\delta^{13}C$ and $\Delta^{14}C$ isotopic signatures in the CO_2 efflux. Previously wet to a moisture content equivalent to 60% of its field capacity, 25 g of soil was placed in hermetic 587 mL glass bottles at a temperature of 25 °C to promote microbial respiration. A four-day pre-incubation was performed to avoid possible distortions in the isotopic signatures associated with the start of the incubation and the air in the bottle was replaced with synthetic (CO_2 free) air. Then, the CO_2 concentration in the bottles was monitored using an infrared gas analyzer (Li-6262). Once a threshold of 1.8 to 2.0 mg C in the bottle headspace was reached, part of the gas was extracted for $\delta^{13}C$ analysis by IRMS. The CO_2 from the remaining headspace air contained in the bottle was extracted using cryogenic separation of CO_2 from other gases (N_2, O_2, and H_2O) on a vacuum line (Trumbore et al., 2016). The purified CO_2 was then heated at 550 °C in the presence of H_2 as a reducing agent and iron powder (Fe) as a catalyst to reduce it to graphite (Steinhof et al., 2017). Finally, this mixture of graphite and iron was analyzed to obtain the $\Delta^{14}C$ signature by AMS (Steinhof et al., 2017).

Additionally, 15 g subsamples of soil from the stratified sampling of 2008 and 2021 were fractionated using the density separation technique (Golchin et al., 1994; Sohi et al., 2001), separating three fractions: free light fraction (fLF), occluded light fraction (oLF) and heavy fraction (HF). The fLF, which represents material with close characteristics to plant input, was obtained by shaking the sample in a sodium polytungstate solution with a density of 1.8 g cm^{-3} and then centrifuging and aspirating the supernatant. The oLF, which constitutes a pool of C physically protected within soil aggregates, was obtained by the same procedure as fLF, but after disrupting the aggregates by sonification (400 J ml^{-1}). The remaining material constitutes the HF and represents the C associated with the soil mineral phase, which has a higher density than the liquid used in the separation procedure (1.8 g cm^{-3}). The HF was dried and finely ground to be analyzed to obtain the $\delta^{13}C$ signature by IRMS and $\Delta^{14}C$ by AMS, as well as the C concentration by dry combustion. In the case of fLF and oLF, a sufficient sample recovery was not achieved to allow their subdivision. Therefore, they were only analyzed for C concentration by dry

https://doi.org/10.5194/egusphere-2025-6451
Preprint. Discussion started: 13 January 2026

combustion and radiocarbon by AMS. The information presented for these two fractions is a descriptive approximation because, due to the small sample mass recovered, it was not possible to make determinations for some plots at some depths. For all three fractions, the recovered weight and their C concentrations were used to calculate the amount of C in each fraction. For those fLF samples for which the determination of C concentration was not available, the average value of all the samples was used. The light fraction (LF) (fLF + oLF), representing particulate material inside and outside aggregates, was obtained as the difference between SOC and HF stock.

2.3. Statistical analysis and modeling

The effect of the agricultural management treatment (CC or R) on total SOC content and fractions (POM-MAOM and fLF-oLF-HF) C content, on the isotopic signatures of $\delta^{13}C$ and $\Delta^{14}C$ by SOC fraction, and on isotopic signatures on CO_2 efflux for each of the depth layers considered, was evaluated by paired t-tests ($p < 0.05$).

To discuss the capacity of integrated crop-pasture systems to stabilize new C in deep layers, we designed a dynamic compartmental model in the form of a system of ordinary differential equations (ODE) to identify which SOC cycling rates and inter-compartment transfers are necessary to explain the C stocks and $\Delta^{14}C$ signatures measured in the R system. These models can be expressed in this general form (Sierra et al., 2012) (Eq. 1):

$$\frac{dC(t)}{dt} = I(t) + A.C(t)$$

Where $C_{(t)}$ is a vector representing the C stock in n pools. $I_{(t)}$ denotes the mass of C entering the system through each of the n pools per unit of time. A is an n x n square matrix containing the output rate constants on its main diagonal and the transfer coefficients between compartments in the off-diagonal entries. This general form can be adapted to represent the radiocarbon flux through a compartmental system (Sierra et al., 2014) as follows (Eq. 2):

$$\frac{d^{14}C(t)}{dt} = I_{14C}(t) + A\,.\ {}^{14}C(t) - \lambda^{14}C(t)$$

Where $I_{14C(t)}$ is a vector of n dimensions containing the radiocarbon inputs to the n pools, $^{14}C_{(t)}$ is the amount of radiocarbon in each compartment n, and λ is the radioactive decay constant (1/8267 y^{-1}).

The model used in this work is an adaptation of the one proposed in González-Sosa et al. (2024), which only represented SOC and radiocarbon dynamics in the 0-20 cm layer. This modification has a scheme of two compartments per depth layer, and C enters each layer through a fast-cycling pool and it is then transferred to a slow-cycling pool in a stabilization process that depends mathematically on the cycling rate of the fast-cycling pool and a transfer coefficient α between both compartments (Fig. 2). The general scheme outlined in equation 1 is expressed for this case as follows (Eq. 3):

https://doi.org/10.5194/egusphere-2025-6451
Preprint. Discussion started: 13 January 2026

$$\frac{dC}{dt} = I \cdot \begin{pmatrix} p_1 \\ 0 \\ p_2 \\ 0 \\ p_3 \\ 0 \\ p_4 \\ 0 \end{pmatrix} \cdot \begin{pmatrix} k_{f1} & 0 & 0 & 0 & 0 & 0 & 0 & 0 \\ \propto_1 k_{f1} & k_{s1} & 0 & 0 & 0 & 0 & 0 & 0 \\ 0 & \beta_i k_{s1}(1-\gamma_j) & k_{f2} & 0 & 0 & 0 & 0 & 0 \\ 0 & \beta_i k_{s1}\gamma_j & \propto_2 k_{f2} & k_{s2} & 0 & 0 & 0 & 0 \\ 0 & 0 & 0 & \beta_i k_{s2}(1-\gamma_j) & k_{f3} & 0 & 0 & 0 \\ 0 & 0 & 0 & \beta_i k_{s2}\gamma_j & \propto_3 k_{f3} & k_{s3} & 0 & 0 \\ 0 & 0 & 0 & 0 & 0 & \beta_i k_{s3}(1-\gamma_j) & k_{f4} & 0 \\ 0 & 0 & 0 & 0 & 0 & \beta_i k_{s3}\gamma_j & \propto_4 k_{f4} & k_{s4} \end{pmatrix} \cdot \begin{pmatrix} C_{fast1} \\ C_{slow1} \\ C_{fast2} \\ C_{slow2} \\ C_{fast3} \\ C_{slow3} \\ C_{fast4} \\ C_{slow4} \end{pmatrix}$$

Where the C enters the system through the labile compartment of each layer and the dynamics down to 80 cm depth is represented in 20 cm intervals. The parameters kfi and ksi represent the output rate constants of the fast and slow pools for each i depth layer, respectively.

The parameters ∝i depict the proportion of C that leaves the fast pool and is transferred to the slow pool at each depth. In addition, the parameters βi represent the proportion of C that leaves the slow pool of a given depth layer and is transferred to the immediately deeper layer. This C flowing into the next layer is divided between the slow and fast pools according to a parameter γ (Fig. 2).

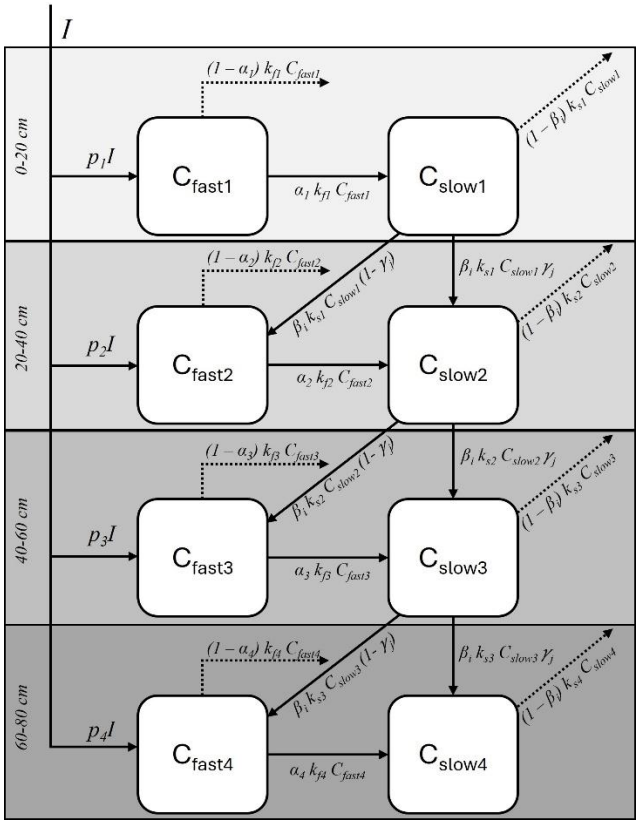

Figure 2. Schematic representation of the model used to interpret the SOC stock and $\Delta^{14}C$ results of the R system. Solid lines represent flows into or between the system pools, and dotted lines represent flows leaving the system.

https://doi.org/10.5194/egusphere-2025-6451
Preprint. Discussion started: 13 January 2026

Since the experimental plots received conventional tillage until 2008 (Baethgen et al., 2021; González-Sosa et al., 2024; Quincke et al., 2019), the 0-20 cm depth was represented as a unique layer, aggregating the corresponding information. Because our focus in this analysis is the dynamics of stable compartments at different depths, we initially assumed the output rate constant of the fast pool (kf) to be constant among layers and equal to 0.651 y^{-1} (González-Sosa et al., 2024). Subsequently, to test this assumption, we tested the effect on the ^{14}C signature, age, and transit time of two linear kf reduction schemes (0.5 and 1% vertical kf reduction per cm of vertical variation), proportionally adjusting the inputs to maintain the estimated stock of the fast pool for each layer. To assess whether the consideration of a vertical movement of pre-aged C is necessary to understand the radiocarbon isotopic signatures measured at depth (Kaiser and Kalbitz, 2012), four scenarios were considered: (1) no vertical movement ($\beta = 0$), (2) 10% ($\beta = 0.1$), (3) 20% ($\beta = 0.2$) and (4) 30% ($\beta = 0.3$) of the C leaving the slow pool of each layer is transferred to the underlying layer. Additionally, we evaluated the effect of three partitioning schemes for these vertical transfers. In the first scheme, the vertical connection occurs exclusively between slow pools ($\gamma = 1$). In the other two schemes, 70% ($\gamma = 0.7$) or 50% ($\gamma = 0.5$) of the C leaving the slow pool of one layer is transferred to the slow pool of the immediately lower layer, while the remaining fraction is transferred to the fast pool of that underlying layer. In order to address the hypotheses related to the dynamics of stable compartments associated with the soil mineral phase, we adjusted the parameters ksi and $\propto i$ to represent the measured MAOM C stocks and $\Delta^{14}C$ signature in the slow compartments at different depths for all the combinations of kf, β, and γ evaluated (30 alternative models).

As proposed by González-Sosa et al. (2024) we assumed the vertical distribution of C inputs to be directly proportional to the vertical distribution of POM C. Based on this and the C input rate reported for this system in the 0-20 cm layer (4.94 Mg ha^{-1} y^{-1}) (González-Sosa et al., 2024) we calculated the C input profile down to 80 cm. Atmospheric radiocarbon information was obtained from Reimer et al. (2013) for the pre-bomb period and from Hua et al. (2022) for the post-bomb period.

Finally, to evaluate the capacity of the deeper layers to incorporate new C into their slow compartments, we increased C inputs to the system by 50% and assessed how much C the different fitted models predicted could be stored in these pools over 50 and 100 years.

2.4. Age and transit time

Once a compartmental model (Fig. 2), which describes the system C dynamics in a deterministic form, is obtained, it can be transformed into a stochastic version to characterize the SOC persistence by calculating its age distribution (Metzler and Sierra, 2018; Sierra et al., 2018). Sierra et al. (2018) define age as the age of the particles or atoms in the system or in its compartments, from the moment they entered the system boundaries to the time of observation, while the transit time is the time elapsed since each atom entered the system until it leaves it.

Once all the alternative models were obtained, we calculated the age of each of their compartments and the transit time of C in the system. A detailed description of the mathematical procedure applied for the calculation of the age distributions,

https://doi.org/10.5194/egusphere-2025-6451
Preprint. Discussion started: 13 January 2026

transit times, as well as for the mean values of each of these variables, can be found in Metzler and Sierra (2018) and Sierra et al. (2018).

3. Results

3.1. Agricultural treatment effect on SOC stock in bulk soil and fractions

As previously reported (Baethgen et al., 2021; González-Sosa et al., 2024), there was a clear effect of the agricultural management treatment on the SOC stock down to 20 cm depth, reaching higher values in the R system compared to the CC system, with significant differences in both the 0-10 cm and 10-20 cm layer and both in 2008 ($p\ value_{0\text{-}10} < 0.010$; $p\ value_{10\text{-}20} = 0.031$) and 2021 ($p\ value_{0\text{-}10} = 0.015$; $p\ value_{10\text{-}20} = 0.030$) (Fig. 3a). The SOC stock down to 20 cm in the R system remained relatively unchanged between years with a stock of 61.17 Mg ha^{-1} in 2008 and 61.73 Mg ha^{-1} in 2021. Regarding the CC system, the SOC stock was 44.53 Mg ha^{-1} in 2008 and 48.31 Mg ha^{-1} in 2021. Focusing on carbon in deeper soil layers, statistically significant differences between agricultural treatments were observed in the 20-40 cm (p value = 0.045) and 60-80 cm (p value = 0.013) layers in 2008, which determined that the SOC stock of the R system in the 20-80 cm layer (80.66 Mg ha^{-1}) was 46% significantly (p value < 0.010) higher than that of the CC system (55.36 Mg ha^{-1}) (Fig. 3a). These significant differences in SOC stocks at depth were lost in the 2021 assessment, essentially due to an increase in SOC stock in the CC system in the 20-40 cm layer and a decrease in stock in the R system in the two deepest layers, with an increase in data dispersion in 2021 (Fig. 3a).

https://doi.org/10.5194/egusphere-2025-6451
Preprint. Discussion started: 13 January 2026

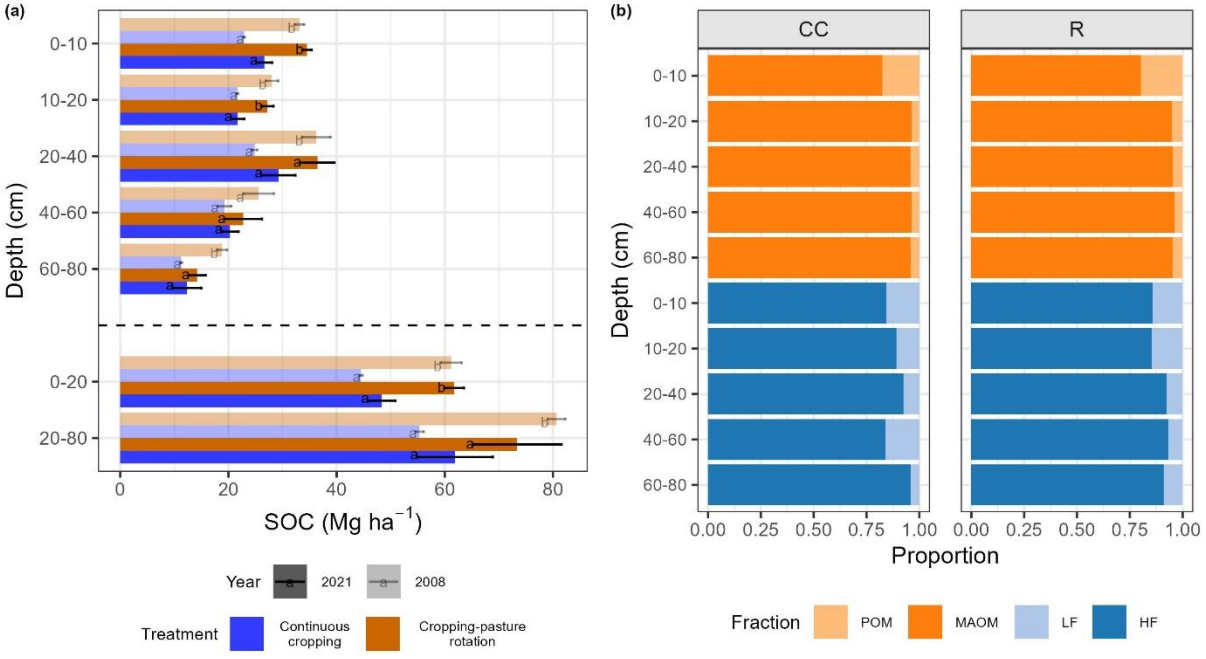

Figure 3. Bulk SOC stock by depth, agricultural treatment, and year of evaluation (a); and proportion of C per fraction according to fractionation method (POM-MAOM and LF-HF) and agricultural treatment in 2021 (b).

There was reasonable agreement between the capacity of the fractionation methods to separate the C associated with the soil mineral phase, represented as HF in the density separation method and as MAOM in the sieving separation method (Fig. 3b). Most of the C in this soil is associated with the mineral phase (HF - MAOM), accounting for more than 80% of the C in the first 10 cm of the soil profile and increasing its relative importance in depth to more than 90% in the last evaluated layer (60-80 cm) in both agricultural management treatments (CC and R). Below 10 cm depth, LF (density separation) fractions comprised a greater proportion of total C compared to POM (size separation), which may be related to the fact that part of the LF contains particulate material that is stabilized within aggregates (oLF), and part of this C (that of size < 2 microns) is contained in the MAOM fraction but not in the POM fraction.

https://doi.org/10.5194/egusphere-2025-6451
Preprint. Discussion started: 13 January 2026

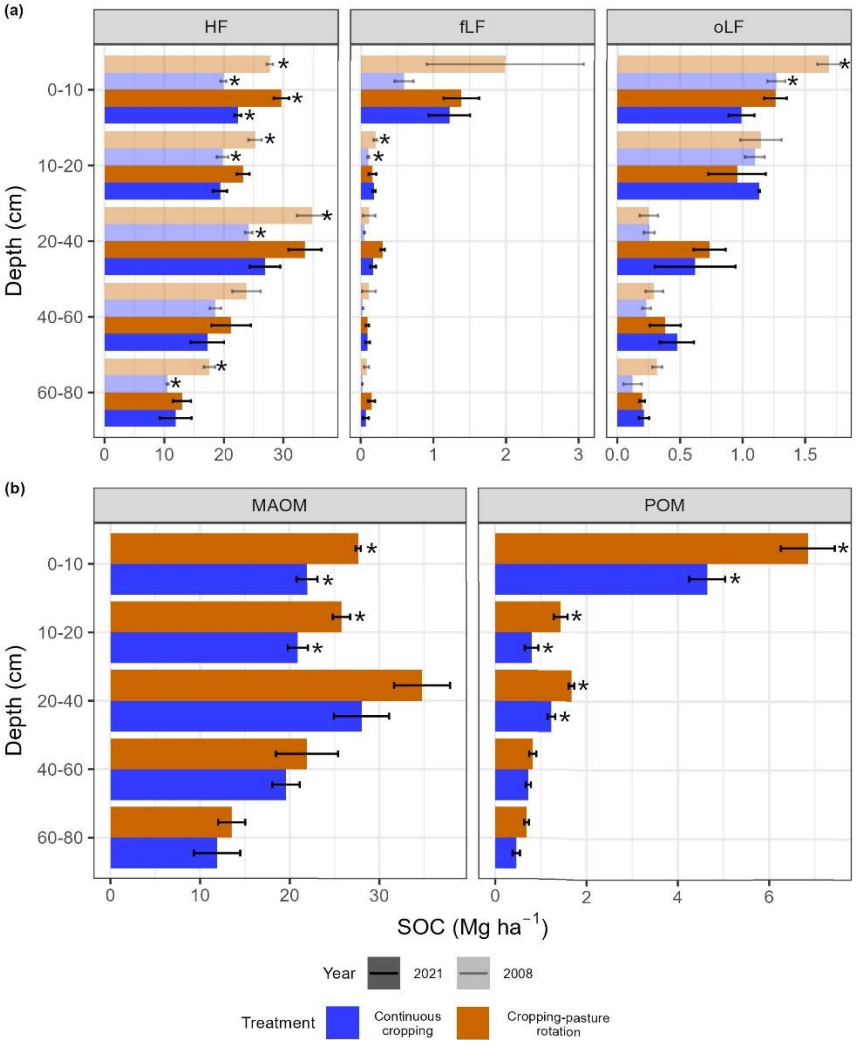

Figure 4. C stock by density fraction according to agricultural treatment and year of evaluation (a) (* indicates significant differences between agricultural treatments in the same year of evaluation); and C stock by sieving fraction according to agricultural treatment in 2021 (b) (* indicates significant differences between agricultural treatments).

Regarding the sieving separation performed in the samples obtained in 2021, González Sosa et al. (2024) had already identified a significantly higher POM C and MAOM C stock in the R system in comparison with the CC system in the 0-20 cm layer. When adding the information from deeper soil horizons we found that, in addition to the differences down to 20 cm, there was also a higher POM C stock in the R system for the 20-40 cm layer (p value = 0.017) (Fig. 4b), though there were no significant differences between treatments in MAOM C stock below 20 cm in 2021 (Fig. 4b). However, with the density separation technique, significant differences between agricultural treatments were observed in almost the entire profile in the HF C stock in 2008, with a higher stock in the R system than in the CC in every layer except 40-60 cm (Fig.

https://doi.org/10.5194/egusphere-2025-6451
Preprint. Discussion started: 13 January 2026

4a). These differences were maintained in 2021 in the first layer and there was a strong statistical trend towards a higher HF C stock in the 10-20 cm layer (p value = 0.075), while significant differences were no longer observed below 20 cm (Fig. 4a), consistent with the results presented for the MAOM C (Fig. 4b) and bulk C (Fig. 3) profile in 2021. In contrast to what was observed for the POM fraction, no significant differences were detected in the C stock of the fLF and oLF in 2021 due to analytical difficulties linked to this technique for handling such small sample sizes in soils that have little particulate material, which led to a large coefficient of variation in the results obtained.

3.2. $\delta^{13}C$ by agricultural treatment, SOC fraction and depth

The SOC fractions showed large differences in $\delta^{13}C$ signatures, with heavier $\delta^{13}C$ in the fractions (MAOM and HF) that tend to have more organic matter associated with the mineral phase, and lighter $\delta^{13}C$ in fractions representing organic C less strongly sorbed to minerals (LF and POM, respectively). These are consistent with a greater degree of microbial resynthesis in the HF and MAOM material. Depth profiles of the MAOM and HF fractions were similar for each of the agricultural treatments, with no statistically significant differences between them, indicating that both SOC fractionation techniques can obtain a fraction with similar characteristics (Fig. 5). Differences in ^{13}C enrichment between more stable compartments (MAOM - HF) with respect to those representing labile material (POM) remained statistically significant at all depths evaluated (Fig. 5; Table A1).

Higher microbial processing was also observed in the MAOM – HF fraction with respect to the oxidized C in the incubation experiment, with the $\delta^{13}C$ signatures of evolved CO_2 significantly different from these soil fractions at all depths except for some comparisons in the two uppermost layers where, in turn, trend differences were observed (Fig. 5; Table A1).

Regarding the effect of the management treatment, greater ^{13}C depletion was observed in the R system, consistent with a lower frequency of C4 photosynthetic cycle crops in the rotation (Fig. 5). Particularly, we observed significant differences between treatments in the SOC fractions associated with the mineral phase (MAOM - HF) in the soil surface layers (down to 40 cm for MAOM and down to 20 cm for HF) (Fig. 5). Although the POM data was much more variable, a strong trend of ^{13}C depletion was observed in the R treatment in 0-10 cm layer ($p=0.050$) and 10-20 cm ($p= 0.059$) layer, and significant in 20-40 cm layer ($p= 0.027$) (Fig. 5). Differences between treatments in the case of incubation-derived CO_2 were much more pronounced, with a greater and significant depletion in ^{13}C in the case of the R system for all layers except for 20-40 and 60-80 cm, in which trends were observed ($p = 0.057$ and $p = 0.060$, respectively) (Fig. 5).

https://doi.org/10.5194/egusphere-2025-6451
Preprint. Discussion started: 13 January 2026

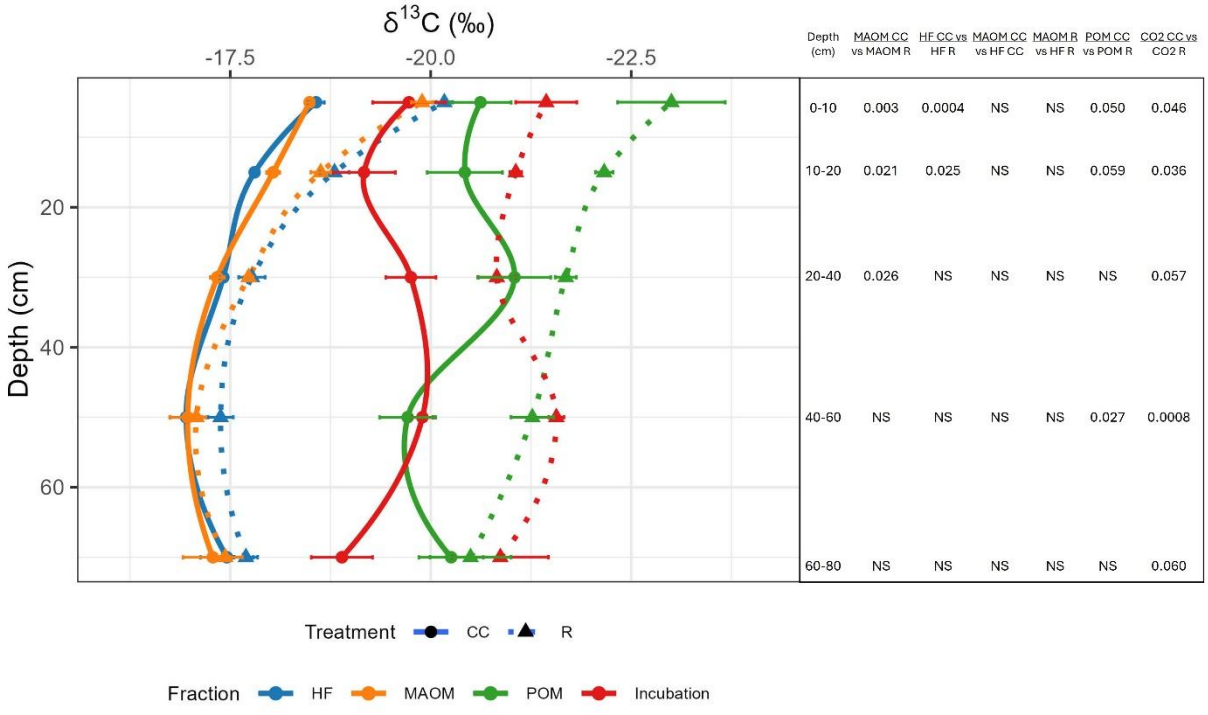

Figure 5. $\delta^{13}C$ isotopic signature of HF, MAOM, POM and CO_2 derived from soil incubations by agricultural treatment in 2021. The table on the right side of the figure presents the p-values for each of the comparisons. Note: NS means not significant.

3.3. $\Delta^{14}C$ by agricultural treatment, SOC fraction and depth

The $\Delta^{14}C$ profiles for the MAOM and HF fractions evaluated in 2021 were very similar for each agricultural treatment (Fig. 6), as was the case for the $\delta^{13}C$ signature (Fig. 5), demonstrating that both fractionation techniques have a similar capacity to separate C associated with the mineral phase. For this isotope, no significant differences were found between the MAOM - HF fractions in the whole profile for both agricultural treatments except for the CC treatment in the 0-10 cm layer, for which the $\Delta^{14}C$ in the HF was significantly lower than in the MAOM ($p = 0.034$) (Fig. 6). The $\Delta^{14}C$ signature in these fractions for both agricultural treatments had a clear pattern of decreasing with depth starting in the case of MAOM with values of -54.43 (R system) and -71.93 (CC system) in the 0-10 cm layer and reaching approximately the same value of -450 in both agricultural treatments in the 60-80 cm layer (Fig. 6). Regarding the treatment effect, there were no significant differences between agricultural managements in the HF or MAOM in 2021 (Fig. 6) and only a significantly higher value of $\Delta^{14}C$ was observed in the R system in the 20-40 cm layer in the HF in 2008 (Fig. 7).

https://doi.org/10.5194/egusphere-2025-6451
Preprint. Discussion started: 13 January 2026

The POM fraction had higher bomb radiocarbon enrichment than the MAOM or HF fractions. This was particularly significant in the first layer (0-10 cm), in which the average $\Delta^{14}C$ value was 2.2 (CC system) and 3.7 (R system), decreasing in depth, but never reaching values lower than -100 (Fig. 6). The $\Delta^{14}C$ values of the POM fraction were significantly higher than those of the MAOM and HF fraction at all depths in the case of the CC treatment (Fig. 6, Table A2). In the case of the R system, significant differences were observed between the C fractions associated with the mineral phase (MAOM and HF) and POM in the 0-10, 20-40 and 60-80 cm layers (Fig. 6, Table A2). No effect of the agricultural treatment on the POM $\Delta^{14}C$ value was observed.

Regarding the LF components obtained by the density separation technique (fLF and oLF), despite not being able to test the effects of the treatments on the isotopic signature due to the loss of samples, a clear trend of the fLF of following the $\Delta^{14}C$ of the atmosphere of the sampling year was observed (Fig. 7). This vertical pattern was independent of the sampling depth and agricultural treatment, with values around +50 in 2008 and around 0 in 2021. In contrast, the oLF exhibited a completely different trend as a function of depth, reaching $\Delta^{14}C$ values closer to the isotopic signature of the atmosphere in the 0-10 cm layer, particularly in 2021, but decreasing rapidly in deeper layers by coupling to the isotopic signature of the HF in both treatments (Fig. 7).

The CO_2 derived from incubation experiments, which represents the labile substrate that is available for microbial respiration, showed a depth profile with higher $\Delta^{14}C$ values than any of the other fractions, evidencing greater enrichment in recently fixed C derived from atmospheric CO_2 since the nuclear-test peak (Fig. 6, Table A2) than other fractions. Differences in respired CO_2 between the agricultural treatments were only significant in the first two layers (0-10 and 10-20 cm), with a higher value in the case of the R system (Fig. 6).

https://doi.org/10.5194/egusphere-2025-6451
Preprint. Discussion started: 13 January 2026

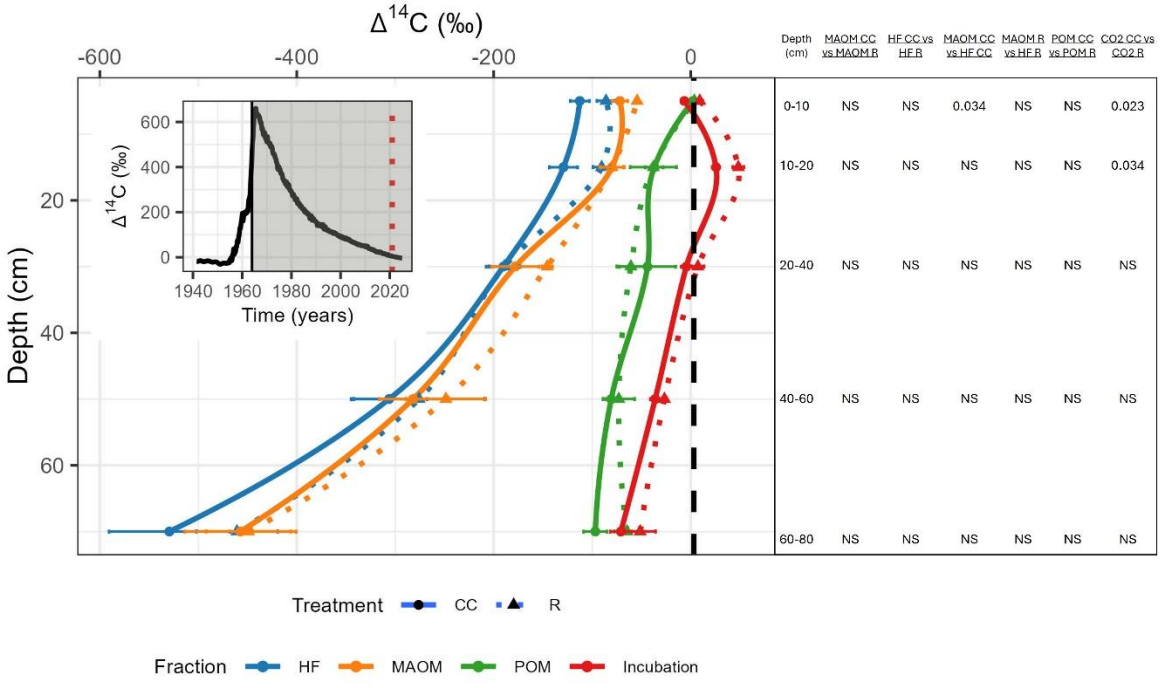

Figure 6. $\Delta^{14}C$ isotopic signature of HF, MAOM, POM and CO_2 derived from soil incubations by agricultural treatment in 2021. The vertical black dashed line corresponds to the $\Delta^{14}C$ atmospheric signature in 2021. $\Delta^{14}C$ in CO_2 down to 20 cm are extracted from González-Sosa (2024). The table on the right side of the figure presents the p-values for each of the comparisons. Note: NS means not significant. The inset graph shows the temporal evolution of the atmospheric $\Delta^{14}C$ signature and its increase during the period of nuclear testing (the gray shaded rectangle indicates the duration of the LTE and the red dashed vertical line the time of sampling of the data presented in the main graph).

https://doi.org/10.5194/egusphere-2025-6451
Preprint. Discussion started: 13 January 2026

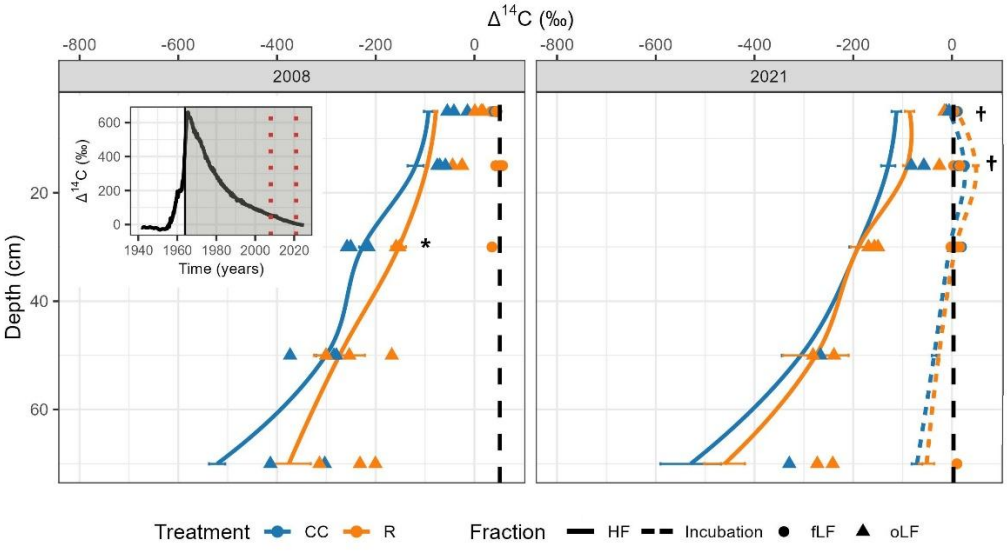

Figure 7. $\Delta^{14}C$ isotopic signature of HF, fLF, and oLF by agricultural treatment and year of evaluation (* indicates significant differences between treatments for HF; † indicates significant differences between treatments for incubation CO_2). Vertical black dashed lines correspond to $\Delta^{14}C$ atmospheric signature of the year of sampling. The inset graph shows the temporal evolution of the atmospheric $\Delta^{14}C$ signature and its increase during the period of nuclear testing (the gray shaded rectangle indicates the duration of the LTE and the red dashed vertical lines the time of sampling of the data presented in the main graph).

3.4. Dynamics of C as a function of depth

Figure 8 shows the average results for C stock (Fig. 8a) and radiocarbon (Fig. 8b) for the 30 modelling scenarios evaluated for the R system. The specific results and parameterization for each run are presented in Supplementary Material S1. The fitted compartmental models were capable of correctly representing the vertical stock distribution of the size fractions (Fig. 8a) and $\Delta^{14}C$ in the MAOM fraction (Fig. 8b). A strong equifinality was observed between the parameter regulating the vertical transfer of SOC between stable compartments (β), the slow compartment decay rates ksi and the ∝i parameters regulating the flux from the fast to the slow pool (stabilization) in each layer. The incremental vertical fluxes (higher values of β) were compensated by higher decay rates of the slow pool and lower stabilization fluxes in each layer to achieve the

https://doi.org/10.5194/egusphere-2025-6451
Preprint. Discussion started: 13 January 2026

same SOC stock estimate and $\Delta^{14}C$ isotopic signature (Table 2). The inclusion of a vertical transfer mechanism for previously stabilized material was not necessary to explain the radiocarbon signatures measured in the stable fractions. By adjusting the ksi output rates and ∝i stabilization coefficients, it was possible to achieve the same estimates of $\Delta^{14}C$ and C stock for all vertical transfer coefficient (β) values considered. Furthermore, transfers from slow pools to deeper fast pools, controlled by combinations of the β and γ parameters, had no significant effect on the model results because these flows were very low in magnitude (due to the low value of the ksi constants), with the dynamics of the fast compartments being essentially governed by the external C inputs and the kfi constants. Moreover, the downward slowdown in the kfi profile had only a minor effect on the radiocarbon signatures and was equifinal with the αi stabilization coefficients. This allowed the reduced kfi to be compensated by a proportional increase in αi, maintaining the C flow into the corresponding slow compartment. All the described equifinalities are visualized in the extremely small standard deviation between model estimates with the alternative 30 combinations of β, γ, and kfi vertical reduction schemes considered (Fig. 8).

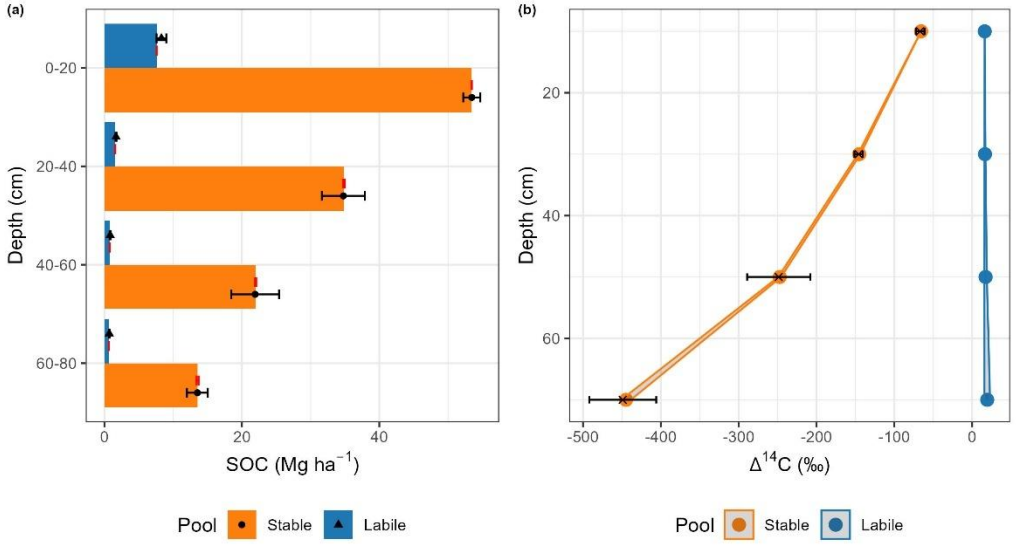

Figure 8. Model predictions (Eq. 3, Fig. 2) of the vertical distribution of the SOC stock (a) and $\Delta^{14}C$ isotopic signature (b) by compartment for the agricultural system R. The labile compartment represents the POM fraction, and the stable compartment represents the MAOM fraction measured in 2021. The dots and black error bars represent the measurements and their standard error. The model predictions in (a) and (b) correspond to the average of the 30 alternative model scenarios considered; the standard deviation among model estimates is represented as red error bars in (a) and as a light ribbon in (b).

https://doi.org/10.5194/egusphere-2025-6451
Preprint. Discussion started: 13 January 2026

Table 2. Model parameters fitted to the R system data, percentage of recent stable SOC and transit time for each alternative vertical transfer scheme considered[(a)].

Depth	β	k_f	γ	k_{si}	$\propto_i$	New stable SOC (%) [(b)]	Transit time
0-20	0	0.651	-	0.001450	0.01520	7.81	19.6 (19.6 – 21.6)
20-40	0	0.651	-	0.000680	0.02370	3.86 (3.84 – 3.86)	
40-60	0	0.651	-	0.000350	0.01580	2.01 (1.97 – 2.01)	
60-80	0	0.651	-	0.000140	0.00450	0.81 (0.78 – 0.81)	
0-20	0.1	0.651	1	0.001450	0.01520	7.81	19.7 (19.6 – 21.7)
20-40	0.1	0.651	1	0.000810	0.02100	3.42 (3.40 – 3.51)	
40-60	0.1	0.651	1	0.000420	0.01300	1.67 (1.65 – 1.90)	
60-80	0.1	0.651	1	0.000174	0.00355	0.62 (0.59 – 0.74)	
0-20	0.2	0.651	1	0.001450	0.01520	7.81	19.7 (19.6 – 21.7)
20-40	0.2	0.651	1	0.000940	0.01780	2.97 (2.95 – 3.33)	
40-60	0.2	0.651	1	0.000525	0.01020	1.32 (1.30 – 1.73)	
60-80	0.2	0.651	1	0.000230	0.00200	0.35 (0.34 – 0.64)	
0-20	0.3	0.651	1	0.001450	0.01520	7.81	19.7 (19.6 – 21.7)
20-40	0.3	0.651	1	0.001050	0.01400	2.4 (2.39 – 3.12)	
40-60	0.3	0.651	1	0.000640	0.00650	0.85 (0.84 – 1.57)	
60-80	0.3	0.651	1	0.000325	0.00050	0.094 (0.090 – 0.49)	

Notes: [(a)] New stable SOC (%) is the percentage of C that entered the slow compartment (~ MAOM) during the period of the experiment (after 1963).

[(b)] To simplify the presentation of the results, only the variation with respect to β is shown, with γ and kfi being constant. When results are presented in parentheses, they correspond to the minimum and maximum values across the 30 runs of the alternative model. Detailed information for each model run is provided in Supplementary Material S1.

The mean age of the SOC increased strongly as it was evaluated at greater depths, being 713 years in the 0-20 cm layer and evolving to more than 5500 years in the deepest layer (60-80 cm) (Fig. 9). The upper layers, which have a more active C exchange with the atmosphere, had a much more right-skewed age distribution with the presence of young C, but a large right tail that was responsible for leveraging the age towards higher values. In contrast, the deeper layers, relatively more isolated from the exchange with the atmosphere, had a less skewed distribution and much higher mean ages. The consideration of a vertical transfer mechanism of previously stabilized material did not have a significant impact on the MAOM C age estimates in the deep layers, with lower average age values estimated as this transfer coefficient increased due to the need to increase the decomposition rates of these compartments to compensate the higher C input associated with this process. Furthermore, consideration of different γ values and kf vertical-reduction schemes within each β level did not have a

https://doi.org/10.5194/egusphere-2025-6451
Preprint. Discussion started: 13 January 2026

significant impact on the age structures either. In any case, the mineral stabilized C ages in deep layers in these soils remained extremely old regardless of the consideration of this vertical movement processes. In this sense, the proportion of C that entered the stable compartment (~ MAOM) since the installation of the experiment declines sharply with depth, decreasing from around 8 % in the 0-20 cm layer to less than 1 % in the deepest layer (Table 2). As a result of the low relative importance of the deep layers in determining the overall dynamics of the profile, the system C transit time remained relatively invariant at a value of approximately 20 years, regardless of β (Table 2). This same pattern is reflected in the limited capacity of the deeper layers (and particularly of the slow compartments) to incorporate new C. When a 50% increase in C inputs to the system is simulated, the model projects, over 50 years, an increase in slow-pool stocks of 0.45 Mg ha^{-1} (1.30%), 0.14 Mg ha^{-1} (0.64%), and 0.029 Mg ha^{-1} (0.21%) in the 20–40, 40–60, and 60–80 cm layers, respectively. Conversely, when this same increase in inputs is projected over 100 years, the corresponding increases are 0.95 Mg ha^{-1} (2.70%), 0.29 Mg ha^{-1} (1.33%), and 0.059 Mg ha^{-1} (0.43%) in these same compartments (Fig. 10).

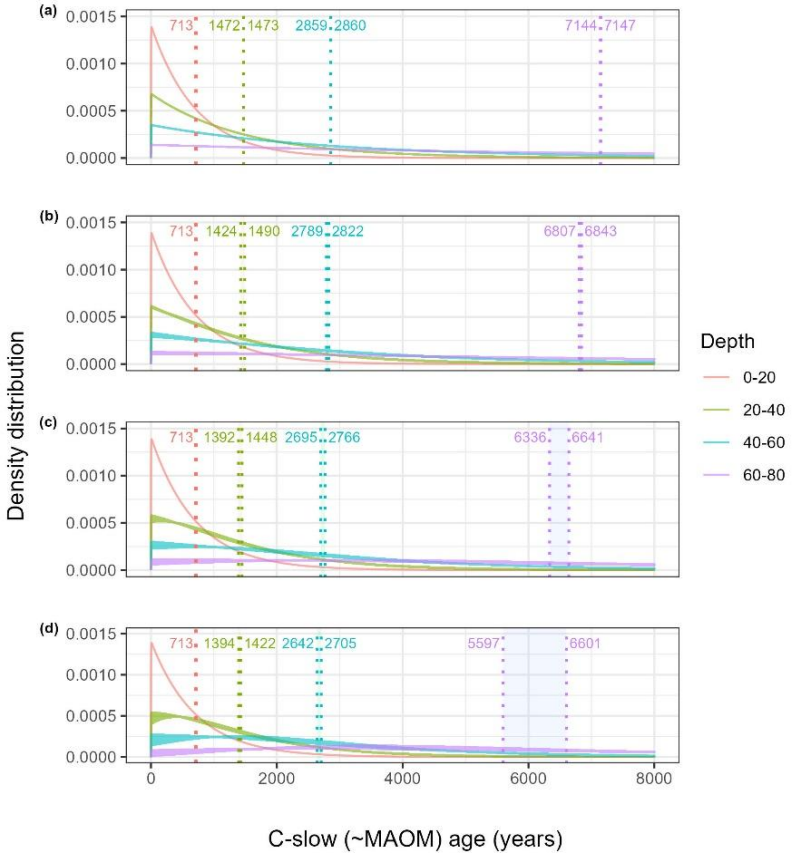

Figure 9. C age distribution in the C-slow (~ MAOM) pool across depth layers under different scenarios of vertical C transfer evaluated in the R system. (a) β = 0, (b) β = 0.1, (c) β = 0.2, (d) β = 0.3. The dark ribbon represents the ensemble of model runs across the different γ values and kf vertical-reduction schemes within each β level. Vertical dotted lines indicate the minimum and maximum mean ages across the corresponding group of simulations for each β scenario.

https://doi.org/10.5194/egusphere-2025-6451
Preprint. Discussion started: 13 January 2026

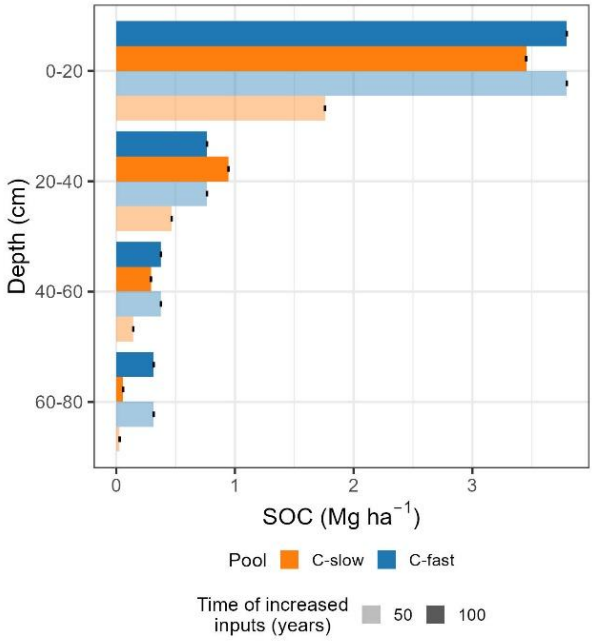

Figure 10. Model predictions of the increase in C stocks in the different compartments resulting from a 50% increase in C inputs for 50 and 100 years. The bars represent the average value for the 30 model scenarios.

4. Discussion

Importance of deep organic C and effect of agricultural treatment

The studied long-term experimental soils are typical in having a significant amount of C below the normally analyzed first 20 cm. Of the total of 135.1 Mg ha^{-1} of C in the R system in 2021 within the top 80 cm of soil, 54% was located between 20-80 cm; while 56% of the total 110.2 Mg ha^{-1} of C in the CC system was found in the same soil depth range (Fig. 3a). These proportions were also similar in the 2008 sampling, with 56.9% and 55.4% of the R and CC system C contained in the 20-80 cm layer, respectively (Fig. 3a), and confirm the relevance of sampling deep soil to avoid underestimation of SOC stocks, as has been claimed in other works (Dietzen et al., 2017; Meersmans et al., 2009; Ward et al., 2016).

From a methodological point of view, we found that the SOC fractionation techniques had similar capacities to separate the C associated with the soil mineral phase -MAOM and HF-, obtaining material with the same characteristics and depth-dependence in $\delta^{13}C$ (Fig. 5) and $\Delta^{14}C$ (Fig. 6) and representing similar proportions of the total SOC (Fig. 3b). However, the small sample size obtained for fLF and oLF in the density separation made this a less useful technique, at least in this type of

https://doi.org/10.5194/egusphere-2025-6451
Preprint. Discussion started: 13 January 2026

soils with little particulate material. The size separation is also much less time consuming and does not involve the expense of the heavy liquid needed for density separation. Incubation of soil and measurement of the released CO_2 shows promise as a way to isolate the isotopic signatures of the most 'labile' fractions, as it is produced directly by microbes. Although similar in ^{14}C signature to the free light fraction, there were also interesting differences (e.g. at 10-20 cm and 40-80 cm) that could indicate that this 'labile' pool is not just limited to unprotected free carbon.

A significant majority of the SOC stock in these soils was contained in compartments representing carbon associated with the mineral phase (MAOM - HF) and which have been characterized in previous works as being linked to high stability or persistence (Lavallee et al., 2020). The proportion of C in these fractions varied from around 80 % in the first 10 cm of soil to more than 90 % in the 60-80 cm layer (Fig. 3b, Fig. 4). Salvo et al. (2010) found similar results regarding the distribution of SOC among fractions associated with different stability in similar soils of Uruguay, with a POM C to SOC ratio that varied between 6.76 and 11.33 % down to 18 cm under different agricultural managements and a very strong vertical stratification, with the proportion of POM decreasing sharply as depth increased in the soil profile. These results are also in line with previous research conducted in "La Estanzuela" LTE, 38 years after its installation (Gentile et al., 2005), who determined that MAOM accounted for more than 90% of the SOC below 20 cm and down to 60 cm.

In our previous work, we identified a significant effect of the incorporation of pastures in agricultural rotations on the SOC stock down to 20 cm depth (González-Sosa et al., 2024). In extending this evaluation to deeper soil layers, we also found a clear effect of the CC system in decreasing the SOC stock in the 20-80 cm layer, which had significantly less C than the R system in 2008 ($p = 0.0012$), though this significance was lost in the 2021 evaluation ($p = 0.35$) (Fig. 3a). In addition to a slight decrease in the C stock in the R system and a slight increase in the C stock in the CC system, which may have determined the result of the comparison in 2021, there is also a noticeable increase in data variability, contributing to the loss of significance (Fig. 3a). In 2008, the experiment experienced some modifications. Conventional tillage was completely replaced by a no-till system, and the sunflower crop was replaced by soybean in the rotation. These modifications could have contributed to the differences observed between the measurements taken in 2008 and 2021.

What do the $\Delta^{14}C$ and $\delta^{13}C$ tell us about the vertical evolution of SOC stability?

The $\Delta^{14}C$ profiles in the MAOM and HF indicate a continuous aging as a function of depth (Fig. 6, Fig. 7). This result is consistent with previous studies showing that C in subsoil horizons is characterized by low ^{14}C activity (Rumpel and Kögel-Knabner, 2011; Scharpenseel and Becker-Heidmann, 1989; Von Fromm et al., 2024). At the same time, it is important to highlight that these fractions, which represent the C associated with the mineral phase, have a high relative importance throughout the profile, which increases in depth, reaching more than 90% of the SOC below 20 cm (Fig. 3b). The reasons why the ^{14}C age of SOC increases with depth are not fully understood (Trumbore, 2009), and it may indicate that SOC stabilization processes at depth occur with greater intensity (Rumpel and Kögel-Knabner, 2011) and/or by the microbial recycling of old, previously stabilized C (Kaiser and Kalbitz, 2012), or due to the fact of lower root inputs and slower

https://doi.org/10.5194/egusphere-2025-6451
Preprint. Discussion started: 13 January 2026

vertical transfers (Sierra et al., 2024; Von Fromm et al., 2024), or to biological factors such as the increasing physical separation between microbes and organic C (Don et al., 2013).

Microbial reprocessing emerges as a mechanism that may explain the stability of the compartments associated with the mineral phase (HF - MAOM) based on the information provided by the vertical trend of the $\delta^{13}C$ signature of the different soil fractions. It was observed that both MAOM and HF are more enriched in ^{13}C than POM in both agricultural treatments. In addition, a clear enrichment in depth of MAOM and HF was visualized except for the last layer, in which the $\delta^{13}C$ signature had a slight decrease (Fig. 5). This would indicate that these fractions are more enriched in C of microbial origin and that the relative importance of this C source (as opposed to fresh plant inputs) would increase with soil depth. Many studies have demonstrated a ^{13}C enrichment of microbial biomass with respect to the processed plant substrate (ŠantRůČková et al., 2000; Wynn et al., 2005). This fractionation occurs due to the favoring of ^{12}C consumption in microbial metabolic processes that generate a residual enrichment in ^{13}C of the unoxidized material. Then, the increasing proportion of SOC derived from microbial biomass would generate the enrichment of the soil organic matter in ^{13}C (Lerch et al., 2011).

Moreover, the results are consistent with previous findings indicating the presence of dynamic SOC at depth (Van Der Voort et al., 2019) due to the decoupling of $\Delta^{14}C$ isotopic signatures between MAOM-HF and that of POM, fLF and incubation-derived CO_2, which becomes more pronounced at greater depth (Fig. 6, Fig. 7). These results show that as depth increases, the SOC that is transferred into stable compartments becomes increasingly isolated from the atmosphere. The dynamics in deep layers would be dominated by an active pool through which most of the SOC entering the system cycles and a progressively smaller proportion flows into the pool associated with the mineral phase as it is evaluated at greater depths.

We had already identified the decoupling between the C pool associated with the mineral fraction and the C inputs to the system through a fast pool as the main reason explaining the elevated surficial SOC content and its high stability in integrated crop-pastures systems with respect to continuous agriculture (González-Sosa et al., 2024). The results of this current work allow us to identify that the process that dominates SOC dynamics in deep layers is not only the same, but that this process becomes more pronounced as we evaluate it further down in the profile. The $\Delta^{14}C$ profile of the MAOM-HF, which can be considered similar to bulk SOC because they make up the largest majority of total SOC, resembles soils of similar characteristics developed over pastures (Mathieu et al., 2015), which highlights the capacity of this type of soils to store and maintain very old C stocks.

Has the integrated crop-pastures system generated a significant incorporation of recent C in deep layers?

The adaptation of the model reported in González-Sosa et al. (2024) aimed at the arable layer to explain SOC dynamics in deep layers (Fig. 2) generated insightful results on the C ages and the implications of considering vertical carbon movement in integrated crop-pasture systems. Kaiser and Kalbitz (2012) proposed the consideration of vertical movement of pre-aged C in the form of DOC to explain the fact that the oldest carbon is found in the newest part of the soil profile (the weathering front). Since we do not have information to characterize the importance of this process as an input to the deep layers, we considered the relevance of evaluating different rates of vertical transfer of previously stabilized C and different schemes for

https://doi.org/10.5194/egusphere-2025-6451
Preprint. Discussion started: 13 January 2026

partitioning these vertical flows into the fast or slow compartments of the underlying layers. We characterized the effect of the variation of this process on the age structure and transit times of SOC in the system. This exercise made evident the strong collinearity between C turnover in each layer and the vertical flow process in explaining the SOC stocks and $\Delta^{14}C$ signature. It is possible to reach the same result regarding C stock and $\Delta^{14}C$ of the MAOM by an increase in the decomposition rate of the stable compartment and decrease of the flux from the labile pool in each layer as increasing rates of vertical C transfer between the stable compartments are considered (Fig. 8, Table 2, Supplementary Material S1). In any case, the variation in the relative importance of this process was of small relevance in determining the age structure of stabilized deep C, which varied from an approximate mean age of 700 years in the 0-20 cm layer to a value ranging from approximately 5500 to 7000 years in the 60-80 cm layer depending on the degree of vertical transfer considered (Fig. 9). These results are consistent with previous reports of SOC ages in deep layers based on ^{14}C measurements (Mathieu et al., 2015; Rumpel et al., 2012; Van Der Voort et al., 2019). Additionally, the inclusion of kfi vertical-reduction schemes, intended to represent potential vertical variation in this decomposition constant, did not result in any meaningful changes to the age structure of stabilized deep C (Fig. 9, Table 2, Supplementary Material S1). Moreover, the consideration of alternative vertical transfer rates had virtually no effect on the transit time, which was approximately 20 years in all cases (Table 2). This value means that each unit mass of new C inputs transits the system in an average period of 20 years or, what is the same, that the average age of C leaving the system is 20 years (Sierra et al., 2017). The joint consideration of the transit time with the high ages of the previously described SOC stable compartments shows us that in these soils most of the C inputs cycle very rapidly through the system and only a very small fraction flows into more stable pools and persists on longer timescales. Furthermore, these results show that the cycling of new carbon occurs mostly in the topsoil, where C cycling is faster. The alternative vertical transfers had no effect on transit times because extremely small amounts of new C are cycled at depth and therefore there is no sensitivity to changes in these transfer rates. Moreover, the assessment of new C allocation under a 50% increase in inputs demonstrates the very limited ability of deep layers to incorporate this additional C, even over a 100-year period (Fig. 10).

The degree of isolation between the SOC fraction associated with the mineral phase (represented by MAOM and HF) increases with depth, which was evident in the important decrease in the $\Delta^{14}C$ signature (Fig. 6, Fig. 7) and the increase in ages described before (Fig. 9). This isolation is explained by the decrease in the C transfer rate from labile to stable compartments as depth increases, the only reason that can explain such negative $\Delta^{14}C$ signatures at depth in the stable fractions. Previous works have suggested the need of a sustained flux of labile C to avoid loss of old C, and it is possible that a large proportion of the C input at depth feeds microbial biomass and prevents destabilization of C that is already stabilized in the mineral phase (Daly et al., 2021; Hicks et al., 2021). The results suggest that as C flows into a stable compartment at depth the probability of it flowing out is progressively lower as depth increases. This could be explained by progressively lower microbial activity due to lower abundance of labile substrates and oxygen (Sun et al., 2021), higher stability of SOC itself due to increased sorption to the mineral phase in a soil that is more distant from saturation in layers with lower SOC stock (Rumpel and Kögel-Knabner, 2011) and/or a process of vertical microbial recycling of previously stabilized C (Kaiser

https://doi.org/10.5194/egusphere-2025-6451
Preprint. Discussion started: 13 January 2026

and Kalbitz, 2012). In this particular case, we could infer that the main mechanism dominating SOC dynamics down to 60 cm would be C association with the soil mineral phase due to an intense microbial reprocessing (progressively older ^{14}C age and higher $\delta^{13}C$), while in the last layer C is highly persistent (high ^{14}C age) despite having less microbial processing (decreased $\delta^{13}C$ signature), possibly due to a lower partial pressure of O_2 (Sun et al., 2021). In any case, the relative contribution of each of the alternative processes to SOC stability at depth remains an open research question (Rumpel and Kögel-Knabner, 2011).

The consideration of all the information regarding the vertical profile of SOC stocks in fractions and isotopic signatures in both agricultural systems (R and CC) and the modeling of the R system suggest that there is no significant capacity of the integrated crop-pasture system to incorporate new C at high rates in stable compartments at depth. These results are consistent with previous research that has shown that deep layers are relatively isolated from C exchange with the atmosphere (Sierra et al., 2024). Therefore, the differences observed in C stocks between agricultural treatments in deep layers (only significant in 2008 evaluation) would be determined by the capacity of R system to avoid the loss of pre-existing old C stored in stable compartments. In this sense, the maintenance of higher stocks of labile C, due to higher C inputs, could prevent the loss of previously stabilized C, which would not become the main substrate for microbial oxidation. This process had already been described in a previous work down to 20 cm depth (González-Sosa et al., 2024), and it is now demonstrated that this mechanism is accentuated as it is evaluated in deeper layers.

5. Conclusions

Through a comparative evaluation of the vertical distribution of SOC stocks and $\Delta^{14}C$ and $\delta^{13}C$ isotopic signatures in fractions of different stability in two agricultural treatments of different intensity of a 60-year long-term experiment, we seek to understand whether integrated crop-pasture rotational systems are an adequate technological strategy to sequester C in deep stable layers.

The soils studied are characterized by having a predominant compartment associated with the mineral phase, constituting more than 90% of the SOC below 20 cm. The $\Delta^{14}C$ isotopic signatures of these compartments are very negative and with depth are increasingly distant from those of the more labile fractions, leading to the conclusion that the stable C, the majority in this type of soil, has a very high degree of isolation from the fresh inputs derived from atmospheric C. The dynamics of the deep SOC is dominated by a very small active pool whose cycling determines that the vast majority of the C inputs return rapidly to the atmosphere. The absence of evidence of new "bomb" C incorporation in deep stable fractions and their extraordinarily high ages indicate that the observed differences between agricultural treatments are due to different loss dynamics between them. The evidence would indicate that integrated crop-pasture rotational systems are not capable of incorporating new C in deep stable compartments at reasonable rates on human time scales, and the capacity to sequester new C following agricultural management changes is concentrated mainly in the surface layers. However, the importance of these systems would lie in their capacity to avoid the loss of deep and long-term stable C, whose formation process involved

https://doi.org/10.5194/egusphere-2025-6451
Preprint. Discussion started: 13 January 2026

time periods of hundreds to thousands of years. Furthermore, these conclusions were not substantially influenced by the consideration of alternative connecting structures between the different soil layers that were used to represent different intensities of pre-aged C vertical movements when representing the information in models.

Appendices

Table A1. p-values of comparisons of $\delta^{13}C$ isotopic signature values between fractions of different stability.

Depth (cm)	MAOM R vs POM R	MAOM CC vs POM CC	HF R vs POM R	HF CC vs POM CC	MAOM R vs Incubation R	MAOM CC vs Incubation CC	HF R vs Incubation R	HF CC vs Incubation CC
0-10	0.039	0.029	0.049	0.026	0.044	0.110	0.071	0.118
10-20	<0.001	0.033	<0.001	0.029	<0.001	0.095	0.003	0.071
20-40	<0.001	0.012	<0.001	0.014	0.004	0.012	<0.001	0.016
40-60	0.003	0.005	<0.001	0.005	<0.001	0.001	<0.001	<0.001
60-80	0.025	0.006	0.024	0.006	0.028	0.039	0.028	0.048

Table A2. p-values of comparisons of $\Delta^{14}C$ isotopic signature values between fractions of different stability.

Depth (cm)	MAOM R vs POM R	MAOM CC vs POM CC	HF R vs POM R	HF CC vs POM CC	MAOM R vs Incubation R	MAOM CC vs Incubation CC	HF R vs Incubation R	HF CC vs Incubation CC
0-10	<0.001	0.009	0.006	0.006	<0.001	0.007	0.005	0.005
10-20	0.210	0.048	0.140	0.009	0.004	0.007	<0.001	0.006
20-40	0.018	0.024	0.004	0.018	<0.001	0.015	0.002	0.005
40-60	0.036	0.026	0.085	0.026	0.032	0.017	0.064	0.018
60-80	0.008	0.020	0.007	0.017	0.006	0.018	0.005	0.015

Code and data availability

Code and data are available for review at the following git repository: https://github.com/maxigon-23/data_and_code_gonzalez_25.git. It will be published with a DOI that can be cited in the publication.

Author contributions

Conceptualization: MGS, CAS, MVP. Data Curation: JAQ, MVP. Formal analysis: MGS. Funding acquisition: MVP. Investigation: MGS. Supervision: MVP, CAS, JAQ, WEB, ST. Writing – original draft preparation: MGS. Writing – review

https://doi.org/10.5194/egusphere-2025-6451
Preprint. Discussion started: 13 January 2026

and editing: MGS, MVP, CAS, JAQ, WEB, ST. All authors have read and agreed to the published version of the manuscript.

Competing interests

The authors declare that they have no conflict of interest.

Financial support

Funding for this work was provided by the cooperation project "Understanding how land management alters C and N cycling in Uruguayan agro-ecosystems" (ANII MPI_ID_2018_1_1008457) between the Instituto Nacional de Investigación Agropecuaria (INIA – Uruguay), the Agencia Nacional de Investigación e Innovación (ANII - Uruguay), and the Max Planck Institute for Biogeochemistry (MPI-BGC - Germany), under the collaboration agreement between INIA- Uruguay and the Max Planck Society (MPG - Germany). The first author received a fellowship from the Comisión Académica de Posgrado (CAP) of the Universidad de la República (Uruguay) and an internship grant from the Agencia Nacional de Investigación e Innovación (ANII - Uruguay) (MOV_CA_2023_1_176321), which were fundamental for the development of this work.

References

Baethgen, W. E., Parton, W. J., Rubio, V., Kelly, R. H., and M. Lutz, S.: Ecosystem dynamics of crop–pasture rotations in a fifty-year field experiment in southern South America: Century model and field results, Soil Sci. Soc. Am. j., 85, 423–437, https://doi.org/10.1002/saj2.20204, 2021.

Baeza, S., Vélez-Martin, E., De Abelleyra, D., Banchero, S., Gallego, F., Schirmbeck, J., Veron, S., Vallejos, M., Weber, E., Oyarzabal, M., Barbieri, A., Petek, M., Guerra Lara, M., Sarrailhé, S. S., Baldi, G., Bagnato, C., Bruzzone, L., Ramos, S., and Hasenack, H.: Two decades of land cover mapping in the Río de la Plata grassland region: The MapBiomas Pampa initiative, RSASE, 28, 100834, https://doi.org/10.1016/j.rsase.2022.100834, 2022.

Balesdent, J., Mariotti, A., and Guillet, B.: Natural 13C abundance as a tracer for studies of soil organic matter dynamics, Soil Biology and Biochemistry, 19, 25–30, https://doi.org/10.1016/0038-0717(87)90120-9, 1987.

Balesdent, J., Basile-Doelsch, I., Chadoeuf, J., Cornu, S., Derrien, D., Fekiacova, Z., and Hatté, C.: Atmosphere–soil carbon transfer as a function of soil depth, Nature, 559, 599–602, https://doi.org/10.1038/s41586-018-0328-3, 2018.

Cambardella, C. A. and Elliott, E. T.: Particulate soil organic-matter changes across a grassland cultivation sequence, Soil Sci. Soc. Am. J., 56, 777–783, 1992.

Castellano, M. J., Mueller, K. E., Olk, D. C., Sawyer, J. E., and Six, J.: Integrating plant litter quality, soil organic matter stabilization, and the carbon saturation concept, Glob Change Biol, 21, 3200–3209, https://doi.org/10.1111/gcb.12982, 2015.

https://doi.org/10.5194/egusphere-2025-6451
Preprint. Discussion started: 13 January 2026

Cates, A. M., Ruark, M. D., Hedtcke, J. L., and Posner, J. L.: Long-term tillage, rotation and perennialization effects on particulate and aggregate soil organic matter, Soil and Tillage Research, 155, 371–380, https://doi.org/10.1016/j.still.2015.09.008, 2016.

Chevallier, T., Woignier, T., Toucet, J., and Blanchart, E.: Organic carbon stabilization in the fractal pore structure of Andosols, Geoderma, 159, 182–188, https://doi.org/10.1016/j.geoderma.2010.07.010, 2010.

Cotrufo, M. F., Soong, J. L., Horton, A. J., Campbell, E. E., Haddix, M. L., Wall, D. H., and Parton, W. J.: Formation of soil organic matter via biochemical and physical pathways of litter mass loss, Nature Geosci, 8, 776–779, https://doi.org/10.1038/ngeo2520, 2015.

Daly, A. B., Jilling, A., Bowles, T. M., Buchkowski, R. W., Frey, S. D., Kallenbach, C. M., Keiluweit, M., Mooshammer, M., Schimel, J. P., and Grandy, A. S.: A holistic framework integrating plant-microbe-mineral regulation of soil bioavailable nitrogen, Biogeochemistry, 154, 211–229, https://doi.org/10.1007/s10533-021-00793-9, 2021.

Dietzen, C. A., Marques, E. R. G., James, J. N., Bernardi, R. H. A., Holub, S. M., and Harrison, R. B.: Response of Deep Soil Carbon Pools to Forest Management in a Highly Productive Andisol, Soil Science Society of America Journal, 81, 970–978, https://doi.org/10.2136/sssaj2016.09.0305, 2017.

Don, A., Rödenbeck, C., and Gleixner, G.: Unexpected control of soil carbon turnover by soil carbon concentration, Environ Chem Lett, 11, 407–413, https://doi.org/10.1007/s10311-013-0433-3, 2013.

Galluzzi, G., Plaza, C., Giannetta, B., Priori, S., and Zaccone, C.: Time and climate roles in driving soil carbon distribution and stability in particulate and mineral-associated organic matter pools, Science of The Total Environment, 963, 178511, https://doi.org/10.1016/j.scitotenv.2025.178511, 2025.

Gentile, R. M., Martino, D. L., and Entz, M. H.: Influence of perennial forages on subsoil organic carbon in a long-term rotation study in Uruguay, Agriculture, Ecosystems & Environment, 105, 419–423, https://doi.org/10.1016/j.agee.2004.05.002, 2005.

Golchin, A., Oades, J., Skjemstad, J., and Clarke, P.: Study of free and occluded particulate organic matter in soils by solid state 13C Cp/MAS NMR spectroscopy and scanning electron microscopy, Soil Res., 32, 285, https://doi.org/10.1071/SR9940285, 1994.

González-Sosa, M., Sierra, C. A., Quincke, J. A., Baethgen, W. E., Trumbore, S., and Pravia, M. V.: High capacity of integrated crop–pasture systems to preserve old soil carbon evaluated in a 60-year-old experiment, SOIL, 10, 467–486, https://doi.org/10.5194/soil-10-467-2024, 2024.

Grahmann, K., Rubio Dellepiane, V., Terra, J. A., and Quincke, J. A.: Long-term observations in contrasting crop-pasture rotations over half a century: Statistical analysis of chemical soil properties and implications for soil sampling frequency, Agric Ecosyst Environ, 287, 106710, https://doi.org/10.1016/j.agee.2019.106710, 2020.

Hicks, L. C., Lajtha, K., and Rousk, J.: Nutrient limitation may induce microbial mining for resources from persistent soil organic matter, Ecology, 102, e03328, https://doi.org/10.1002/ecy.3328, 2021.

Hua, Q., Turnbull, J. C., Santos, G. M., Rakowski, A. Z., Ancapichún, S., De Pol-Holz, R., Hammer, S., Lehman, S. J., Levin, I., Miller, J. B., Palmer, J. G., and Turney, C. S. M.: Atmospheric radiocarbon for the period 1950–2019, Radiocarbon, 64, 723–745, https://doi.org/10.1017/RDC.2021.95, 2022.

INIA GRAS: Unidad de Agro-clima y Sistemas de información (GRAS), 2023.

https://doi.org/10.5194/egusphere-2025-6451
Preprint. Discussion started: 13 January 2026

IPCC: Climate change 2014 synthesis report. Contribution of Working Groups I, II and III to the Fifth Assessment Report of the Intergovernmental Panel on Climate Change [Core Writing Team, R.K. Pachauri and L.A. Meyer (eds.)]., IPCC: Geneva, Szwitzerland, 151, 2014.

IPCC: Global Warming of 1.5°C: IPCC Special Report on Impacts of Global Warming of 1.5°C above Pre-industrial Levels in Context of Strengthening Response to Climate Change, Sustainable Development, and Efforts to Eradicate Poverty, 1st ed., Cambridge University Press, https://doi.org/10.1017/9781009157940, 2022.

Jenkinson, D. S.: The turnover of organic carbon and nitrogen in soil, Phil. Trans. R. Soc. Lond. B, 329, 361–368, https://doi.org/10.1098/rstb.1990.0177, 1990.

Kaiser, K. and Kalbitz, K.: Cycling downwards – dissolved organic matter in soils, Soil Biology and Biochemistry, 52, 29–32, https://doi.org/10.1016/j.soilbio.2012.04.002, 2012.

Keiluweit, M., Wanzek, T., Kleber, M., Nico, P., and Fendorf, S.: Anaerobic microsites have an unaccounted role in soil carbon stabilization, Nat Commun, 8, 1771, https://doi.org/10.1038/s41467-017-01406-6, 2017.

Kleber, M., Nico, P. S., Plante, A., Filley, T., Kramer, M., Swanston, C., and Sollins, P.: Old and stable soil organic matter is not necessarily chemically recalcitrant: implications for modeling concepts and temperature sensitivity, Glob Chang Biol, 17, 1097–1107, https://doi.org/10.1111/j.1365-2486.2010.02278.x, 2011.

Lal, R.: Tillage effects on soil degradation, soil resilience, soil quality, and sustainability, Soil and tillage Research, 27, 1–8, 1993.

Lavallee, J. M., Soong, J. L., and Cotrufo, M. F.: Conceptualizing soil organic matter into particulate and mineral-associated forms to address global change in the 21st century, Glob Change Biol, 26, 261–273, https://doi.org/10.1111/gcb.14859, 2020.

Lerch, T. Z., Nunan, N., Dignac, M.-F., Chenu, C., and Mariotti, A.: Variations in microbial isotopic fractionation during soil organic matter decomposition, Biogeochemistry, 106, 5–21, https://doi.org/10.1007/s10533-010-9432-7, 2011.

Mathieu, J. A., Hatté, C., Balesdent, J., and Parent, É.: Deep soil carbon dynamics are driven more by soil type than by climate: a worldwide meta-analysis of radiocarbon profiles, Global Change Biology, 21, 4278–4292, https://doi.org/10.1111/gcb.13012, 2015.

Meersmans, J., Van Wesemael, B., De Ridder, F., Fallas Dotti, M., De Baets, S., and Van Molle, M.: Changes in organic carbon distribution with depth in agricultural soils in northern Belgium, 1960–2006, Global Change Biology, 15, 2739–2750, https://doi.org/10.1111/j.1365-2486.2009.01855.x, 2009.

Metzler, H. and Sierra, C. A.: Linear Autonomous Compartmental Models as Continuous-Time Markov Chains: Transit-Time and Age Distributions, Math Geosci, 50, 1–34, https://doi.org/10.1007/s11004-017-9690-1, 2018.

Minasny, B., Malone, B. P., McBratney, A. B., Angers, D. A., Arrouays, D., Chambers, A., Chaplot, V., Chen, Z.-S., Cheng, K., Das, B. S., Field, D. J., Gimona, A., Hedley, C. B., Hong, S. Y., Mandal, B., Marchant, B. P., Martin, M., McConkey, B. G., Mulder, V. L., O'Rourke, S., Richer-de-Forges, A. C., Odeh, I., Padarian, J., Paustian, K., Pan, G., Poggio, L., Savin, I., Stolbovoy, V., Stockmann, U., Sulaeman, Y., Tsui, C.-C., Vågen, T.-G., van Wesemael, B., and Winowiecki, L.: Soil carbon 4 per mille, Geoderma, 292, 59–86, https://doi.org/10.1016/j.geoderma.2017.01.002, 2017.

Poeplau, C., Don, A., Six, J., Kaiser, M., Benbi, D., Chenu, C., Cotrufo, M. F., Derrien, D., Gioacchini, P., Grand, S., Gregorich, E., Griepentrog, M., Gunina, A., Haddix, M., Kuzyakov, Y., Kühnel, A., Macdonald, L. M., Soong, J., Trigalet,

https://doi.org/10.5194/egusphere-2025-6451
Preprint. Discussion started: 13 January 2026

S., Vermeire, M.-L., Rovira, P., van Wesemael, B., Wiesmeier, M., Yeasmin, S., Yevdokimov, I., and Nieder, R.: Isolating organic carbon fractions with varying turnover rates in temperate agricultural soils – A comprehensive method comparison, Soil Biology and Biochemistry, 125, 10–26, https://doi.org/10.1016/j.soilbio.2018.06.025, 2018.

Pravia, M. V., Kemanian, A. R., Terra, J. A., Shi, Y., Macedo, I., and Goslee, S.: Soil carbon saturation, productivity, and carbon and nitrogen cycling in crop-pasture rotations, Agric. Syst., 171, 13–22, https://doi.org/10.1016/j.agsy.2018.11.001, 2019.

Quincke, J., Ciganda, V., Sawchik, J., Fernández, E., Hirigoyen, D., Sotelo, D., Restaino, E., and Lapetina, J.: Rotaciones cultivos pasturas INIA La Estanzuela: Aprendiendo del experimento más antiguo de Latinoamérica, 59, 46–60, 2019.

Reimer, P. J., Bard, E., Bayliss, A., Beck, J. W., Blackwell, P. G., Ramsey, C. B., Buck, C. E., Cheng, H., Edwards, R. L., Friedrich, M., Grootes, P. M., Guilderson, T. P., Haflidason, H., Hajdas, I., Hatté, C., Heaton, T. J., Hoffmann, D. L., Hogg, A. G., Hughen, K. A., Kaiser, K. F., Kromer, B., Manning, S. W., Niu, M., Reimer, R. W., Richards, D. A., Scott, E. M., Southon, J. R., Staff, R. A., Turney, C. S. M., and Van Der Plicht, J.: IntCal13 and Marine13 Radiocarbon Age Calibration Curves 0–50,000 Years cal BP, Radiocarbon, 55, 1869–1887, https://doi.org/10.2458/azu_js_rc.55.16947, 2013.

Rubio, V., Pérez Bidegain, M., Beretta, A., Barolin, E., and Quincke, A.: Impacto de propiedades físico-químicas en la estabilidad estructural de Molisoles, Ciencia del suelo, 37, 367–371, 2019.

Rui, Y., Jackson, R. D., Cotrufo, M. F., Sanford, G. R., Spiesman, B. J., Deiss, L., Culman, S. W., Liang, C., and Ruark, M. D.: Persistent soil carbon enhanced in Mollisols by well-managed grasslands but not annual grain or dairy forage cropping systems, Proc. Natl. Acad. Sci. U.S.A., 119, e2118931119, https://doi.org/10.1073/pnas.2118931119, 2022.

Rumpel, C. and Kögel-Knabner, I.: Deep soil organic matter—a key but poorly understood component of terrestrial C cycle, Plant Soil, 16, 2011.

Rumpel, C., Chabbi, A., and Marschner, B.: Carbon Storage and Sequestration in Subsoil Horizons: Knowledge, Gaps and Potentials, in: Recarbonization of the Biosphere, edited by: Lal, R., Lorenz, K., Hüttl, R. F., Schneider, B. U., and Von Braun, J., Springer Netherlands, Dordrecht, 445–464, https://doi.org/10.1007/978-94-007-4159-1_20, 2012.

Rumpel, C., Amiraslani, F., Chenu, C., Garcia Cardenas, M., Kaonga, M., Koutika, L.-S., Ladha, J., Madari, B., Shirato, Y., Smith, P., Soudi, B., Soussana, J.-F., Whitehead, D., and Wollenberg, E.: The 4p1000 initiative: Opportunities, limitations and challenges for implementing soil organic carbon sequestration as a sustainable development strategy, Ambio, 49, 350–360, https://doi.org/10.1007/s13280-019-01165-2, 2019.

Salvo, L., Hernández, J., and Ernst, O.: Distribution of soil organic carbon in different size fractions, under pasture and crop rotations with conventional tillage and no-till systems, Soil and Tillage Research, 109, 116–122, https://doi.org/10.1016/j.still.2010.05.008, 2010.

ŠantRůČková, H., Bird, M. I., and Lloyd, J.: Microbial processes and carbon-isotope fractionation in tropical and temperate grassland soils, Functional Ecology, 14, 108–114, https://doi.org/10.1046/j.1365-2435.2000.00402.x, 2000.

Scharpenseel, H.-W. and Becker-Heidmann, P.: Shifts in 14C Patterns of Soil Profiles Due to Bomb Carbon, Including Effects of Morphogenetic and Turbation Processes, Radiocarbon, 31, 627–636, https://doi.org/10.1017/S0033822200012224, 1989.

Schmidt, M. W., Torn, M. S., Abiven, S., Dittmar, T., Guggenberger, G., Janssens, I. A., Kleber, M., Kögel-Knabner, I., Lehmann, J., and Manning, D. A.: Persistence of soil organic matter as an ecosystem property, Nature, 478, 49–56, https://doi.org/10.1038/nature10386, 2011.

https://doi.org/10.5194/egusphere-2025-6451
Preprint. Discussion started: 13 January 2026

Schrumpf, M., Kaiser, K., Guggenberger, G., Persson, T., Kögel-Knabner, I., and Schulze, E.-D.: Storage and stability of organic carbon in soils as related to depth, occlusion within aggregates, and attachment to minerals, Biogeosciences, 10, 1675–1691, https://doi.org/10.5194/bg-10-1675-2013, 2013.

Schuur, E. A. G., Carbone, M. S., Hicks Pries, C. E., Hopkins, F. M., and Natali, S. M.: Radiocarbon in Terrestrial Systems, in: Radiocarbon and Climate Change, edited by: Schuur, E. A. G., Druffel, E., and Trumbore, S. E., Springer International Publishing, Cham, 167–220, https://doi.org/10.1007/978-3-319-25643-6_6, 2016.

Sierra, C. A., Müller, M., and Trumbore, S. E.: Models of soil organic matter decomposition: the SoilR package, version 1.0, Geosci. Model Dev., 5, 1045–1060, https://doi.org/10.5194/gmd-5-1045-2012, 2012.

Sierra, C. A., Müller, M., and Trumbore, S. E.: Modeling radiocarbon dynamics in soils: SoilR version 1.1, Biogeosciences, https://doi.org/10.5194/gmdd-7-3161-2014, 2014.

Sierra, C. A., Müller, M., Metzler, H., Manzoni, S., and Trumbore, S. E.: The muddle of ages, turnover, transit, and residence times in the carbon cycle, Glob Change Biol, 23, 1763–1773, https://doi.org/10.1111/gcb.13556, 2017.

Sierra, C. A., Hoyt, A. M., He, Y., and Trumbore, S. E.: Soil Organic Matter Persistence as a Stochastic Process: Age and Transit Time Distributions of Carbon in Soils, Global Biogeochem. Cycles, 32, 1574–1588, https://doi.org/10.1029/2018GB005950, 2018.

Sierra, C. A., Ahrens, B., Bolinder, M. A., Braakhekke, M. C., Von Fromm, S., Kätterer, T., Luo, Z., Parvin, N., and Wang, G.: Carbon sequestration in the subsoil and the time required to stabilize carbon for climate change mitigation, Global Change Biology, 30, e17153, https://doi.org/10.1111/gcb.17153, 2024.

Six, J., Callewaert, P., Lenders, S., De Gryze, S., Morris, S. J., Gregorich, E. G., Paul, E. A., and Paustian, K.: Measuring and Understanding Carbon Storage in Afforested Soils by Physical Fractionation, Soil Science Soc of Amer J, 66, 1981–1987, https://doi.org/10.2136/sssaj2002.1981, 2002.

Sohi, S. P., Mahieu, N., Arah, J. R. M., Powlson, D. S., Madari, B., and Gaunt, J. L.: A Procedure for Isolating Soil Organic Matter Fractions Suitable for Modeling, Soil Sci. Soc. Am. J., 65, 1121–1128, https://doi.org/10.2136/sssaj2001.6541121x, 2001.

Soil Survey Staff: Keys to soil taxonomy, 12th ed., United States Department of Agriculture, Natural Resources Conservation Service, Washington DC, USA., 2014.

Steinhof, A., Altenburg, M., and Machts, H.: Sample Preparation at the Jena ^{14} C Laboratory, Radiocarbon, 59, 815–830, https://doi.org/10.1017/RDC.2017.50, 2017.

Sun, T., Wang, Y., Lucas-Borja, M. E., Jing, X., and Feng, W.: Divergent vertical distributions of microbial biomass with soil depth among groups and land uses, Journal of Environmental Management, 292, 112755, https://doi.org/10.1016/j.jenvman.2021.112755, 2021.

Torn, M. S., Swanston, C. W., Castanha, C., and Trumbore, S. E.: Storage and Turnover of Organic Matter in Soil, in: Biophysico-Chemical Processes Involving Natural Nonliving Organic Matter in Environmental Systems, edited by: Senesi, N., Xing, B., and Huang, P. M., John Wiley & Sons, Inc., Hoboken, NJ, USA, 219–272, https://doi.org/10.1002/9780470494950.ch6, 2009.

Trumbore, S.: Age of Soil Organic Matter and Soil Respiration: Radiocarbon Constraints on Belowground C Dynamics, Ecol. Appl., 10, 399–411, https://doi.org/10.1890/1051-0761(2000)010%255B0399:AOSOMA%255D2.0.CO;2, 2000.

https://doi.org/10.5194/egusphere-2025-6451
Preprint. Discussion started: 13 January 2026

Trumbore, S.: Radiocarbon and Soil Carbon Dynamics, Annu. Rev. Earth Planet. Sci., 37, 47–66, https://doi.org/10.1146/annurev.earth.36.031207.124300, 2009.

Trumbore, S. E. and Zheng, S.: Comparison of Fractionation Methods for Soil Organic Matter ^{14}C Analysis, Radiocarbon, 38, 219–229, https://doi.org/10.1017/S0033822200017598, 1996.

Trumbore, S. E., Xu, X., Santos, G. M., Czimczik, C. I., Beaupré, S. R., Pack, M. A., Hopkins, F. M., Stills, A., Lupascu, M., and Ziolkowski, L.: Preparation for Radiocarbon Analysis, edited by: Schuur, E. A. G., Druffel, E., and Trumbore, S. E., Radiocarbon and Climate Change: Mechanisms, Applications and Laboratory Techniques, 279–315, 2016.

Van Der Voort, T. S., Mannu, U., Hagedorn, F., McIntyre, C., Walthert, L., Schleppi, P., Haghipour, N., and Eglinton, T. I.: Dynamics of deep soil carbon – insights from 14C time series across a climatic gradient, Biogeosciences, 16, 3233–3246, https://doi.org/10.5194/bg-16-3233-2019, 2019.

Von Fromm, S. F., Hoyt, A. M., Sierra, C. A., Georgiou, K., Doetterl, S., and Trumbore, S. E.: Controls and relationships of soil organic carbon abundance and persistence vary across pedo-climatic regions, Global Change Biology, 30, e17320, https://doi.org/10.1111/gcb.17320, 2024.

Ward, S. E., Smart, S. M., Quirk, H., Tallowin, J. R. B., Mortimer, S. R., Shiel, R. S., Wilby, A., and Bardgett, R. D.: Legacy effects of grassland management on soil carbon to depth, Global Change Biology, 22, 2929–2938, https://doi.org/10.1111/gcb.13246, 2016.

Wynn, J. G., Bird, M. I., and Wong, V. N. L.: Rayleigh distillation and the depth profile of 13C/12C ratios of soil organic carbon from soils of disparate texture in Iron Range National Park, Far North Queensland, Australia, Geochimica et Cosmochimica Acta, 69, 1961–1973, https://doi.org/10.1016/j.gca.2004.09.003, 2005.

Xu, X., Pei, J., Xu, Y., and Wang, J.: Soil organic carbon depletion in global Mollisols regions and restoration by management practices: a review, J Soils Sediments, 20, 1173–1181, https://doi.org/10.1007/s11368-019-02557-3, 2020.